2010

On the dynamics of canopy resistance: Generalized linear estimation and relationships with primary micrometeorological variables

Suat Irmak
University of Nebraska-Lincoln, suat.irmak@unl.edu

Denis Mutiibwa
University of Nebraska-Lincoln

On the dynamics of canopy resistance: Generalized linear estimation and relationships with primary micrometeorological variables

Suat Irmak[1] and Denis Mutiibwa[1]

Received 4 August 2009; revised 29 January 2010; accepted 22 February 2010; published 13 August 2010.

[1] The 1-D and single layer combination-based energy balance Penman-Monteith (PM) model has limitations in practical application due to the lack of canopy resistance (r_c) data for different vegetation surfaces. r_c could be estimated by inversion of the PM model if the actual evapotranspiration (E_{Ta}) rate is known, but this approach has its own set of issues. Instead, an empirical method of estimating r_c is suggested in this study. We investigated the relationships between primary micrometeorological parameters and r_c and developed seven models to estimate r_c for a nonstressed maize canopy on an hourly time step using a generalized-linear modeling approach. The most complex r_c model uses net radiation (R_n), air temperature (T_a), vapor pressure deficit (VPD), relative humidity (RH), wind speed at 3 m (u_3), aerodynamic resistance (r_a), leaf area index (LAI), and solar zenith angle (Θ). The simplest model requires R_n, T_a, and RH. We present the practical implementation of all models via experimental validation using scaled up r_c data obtained from the dynamic diffusion porometer-measured leaf stomatal resistance through an extensive field campaign in 2006. For further validation, we estimated E_{Ta} by solving the PM model using the modeled r_c from all seven models and compared the PM E_{Ta} estimates with the Bowen ratio energy balance system (BREBS)-measured E_{Ta} for an independent data set in 2005. The relationships between hourly r_c versus T_a, RH, VPD, R_n, incoming shortwave radiation (R_s), u_3, wind direction, LAI, Θ, and r_a were presented and discussed. We demonstrated the negative impact of exclusion of LAI when modeling r_c, whereas exclusion of r_a and Θ did not impact the performance of the r_c models. Compared to the calibration results, the validation root mean square difference between observed and modeled r_c increased by 5 s m^{-1} for all r_c models developed, ranging from 9.9 s m^{-1} for the most complex model to 22.8 s m^{-1} for the simplest model, as compared with the observed r_c. The validation r^2 values were close to 0.70 for all models, and the modeling efficiency ranged from 0.61 for the most complex model to −1.09 for the simplest model. There was a strong agreement between the BREBS-measured and the PM-estimated E_{Ta} using modeled r_c. These findings can aid in the selection of a suitable model based on the availability and quality of the input data to predict r_c for one-step application of the PM model to estimate E_{Ta} for a nonstressed maize canopy.

Citation: Irmak, S., and D. Mutiibwa (2010), On the dynamics of canopy resistance: Generalized linear estimation and relationships with primary micrometeorological variables, *Water Resour. Res.*, *46*, W08526, doi:10.1029/2009WR008484.

1. Introduction and Background

[2] Physically and combination-based calculations of actual evapotranspiration (E_{Ta}) [i.e., Penman-Monteith [*Monteith*, 1965]] require quantification of the canopy resistance (r_c). Water vapor from vegetative surfaces has to overcome diffusive resistances as it transpires from the stomatal cavities and through the boundary layer to the atmosphere. The term stomatal resistance (r_s) is used to describe the diffusive resistance to water vapor flux from the epidermal stomatal cavities to the leaf surface. Soil moisture also encounters capillary resistance as it evaporates and diffuses from the soil surface to the microclimate. *Monteith* [1965] conceptualized these resistances and combined them into a r_c term which was originally integrated into the Penman-Monteith (PM) "big leaf" model as an extension of a combination-based model by *Penman* [1948]. *Monteith* [1965] noted that r_c is not purely physiological because it includes the external resistance across the boundary layer, which are variable with wind speed and other environmental factors. While conceptually innovative, the gap of knowledge between the single leaf and plant canopy created difficulty in the development of reliable methods to combine the dynamic diffusive processes in the stomata and the boundary layer into a simple model [*Lhomme*, 1991].

[1]Department of Biological Systems Engineering, University of Nebraska-Lincoln, Lincoln, Nebraska, USA.

0043-1397/10/2009WR008484

[3] Quantifying r_c has been the subject of many studies. Applying the Ohm's law analogy, *Monteith* [1965] illustrated r_c as being proportional to the vapor pressure difference (potential difference) between the leaf surface and the microclimate surrounding the canopy and inversely proportional to the water vapor flux [current, $e_s(T)$] and leaf temperature (T_L). In the PM method, the surface temperature and humidity are eliminated by combining the bulk aerodynamic and heat balance relationships [*Webb*, 1984]. Although the analogy is physically sound, it is practically difficult to quantify T_L and $e_s(T)$ at a specific level within the canopy continuously. The spatial and temporal variation in $e_s(T)$ and T_L in the canopy further compound the complexity of using the analogy. The complexity to comprehend and quantify r_c has compelled researchers [*Tanner*, 1963; *Brutsaert*, 1982] to even question its physical significance. *Philip* [1966] suggested, "canopy resistance is an artifact of a somewhat unrealistic analysis, and its physiological significance is questionable." Despite the lack of a practical and physically sound methodology to estimate r_c for a variety of vegetation, climatic, soil water status, and management conditions, the PM method has been widely regarded by the scientific community as one of the most robust and accurate approaches to quantify evaporative losses from plant communities.

[4] Considering the simpler Monteith's one-layer and 1-D "big leaf" approach, *Szeicz and Long* [1969] introduced a widely applied procedure to estimate r_c as a quotient of mean r_s and effective green leaf area index (LAI). They assumed that when soil evaporation is negligible r_c represents effective r_s of all leaves acting as resistances in parallel. *Jarvis* [1981] proposed a novel approach for estimating r_c as the sum of the r_s values of all individual leaves in an imaginary column through the canopy standing on a unit area of ground. This proposal was further investigated by *Leverenz et al.* [1982], *Whitehead et al.* [1984], and *Beadle et al.* [1985] toward developing a multilayer approach. A multilayer approach, independent of wind speed, to estimate r_c was presented by *Lhomme* [1991], and the resulting observed r_c value was considered as a good physiological parameter when soil evaporation is negligible. Another multilayer model of r_c represents and captures the radiant energy at several levels in the canopy and the heat exchanges between leaves and air at these levels in terms of the layer average r_s to water vapor flow and leaf boundary layer resistance to water vapor and sensible heat flow [*Shuttleworth*, 2006]. *Juang et al.* [2008] present the results of extensive analyses and interpretation of first-, second-, and third-order closure models to investigate the radiative and turbulence transfer scheme for within and above canopy scalar transfer. Using a fixed r_s value for well-watered plants has also been suggested [*Monteith*, 1965; *Szeicz and Long*, 1969]. However, computing r_c by simply averaging different layers of r_s can be problematic since $e_s(T)$ and vapor pressure deficit (VPD) are dynamic within the canopy, and changes in VPD and $e_s(T)$ would influence r_c. Another foremost methodology to estimate r_c and evaporative losses from plant communities is the sap flux method. This method provides a unique intermediate between leaf and whole canopy level measurements, and it has been shown recently that the sap flux and porometer measurements of stomatal and canopy conductance match well [*Meinzer and Grantz*, 1990; *Meinzer et al.*, 1995; *Saliendra et al.*, 1995; *Sperry*, 2000; *Ewers et al.*, 2007]. Furthermore, research on the VPD and soil moisture response of r_c has been shown to match plant hydraulic theory well [*Whitehead*, 1998; *Oren et al.*, 1999; *Ewers et al.*, 2005; *Franks*, 2004], which is recently being integrated into models of transpiration and by implication of E_{Ta} [*Mackay et al.*, 2003; *Pataki and Oren*, 2003; *Ewers et al.*, 2008]. The plant hydraulic theory and its functions, especially the relationship between soil water, xylem properties, and leaf conductance (g), are presented and discussed in detail by *Meinzer and Grantz* [1990], *Sperry et al.* [1993], *Sperry and Pockman* [1993], *Saliendra et al.* [1995], *Sperry et al.* [1998], *Sperry* [2000], and *Franks* [2004]. The sap flux method has an advantage over the porometric measurements of g in that it does not disturb the leaf boundary layer. However, the practical application of the sap flux method is somewhat more widespread for woody vegetation rather than agronomic plants.

[5] Following the milestone multiplicative empirical r_s model from the study of the response of r_s to environmental variables by *Jarvis* [1976], a different approach to estimating r_c is the scaling-up of measured or estimated r_s to r_c. The fortunate capability of porometers to measure r_s has made the "scaling-up" approach a motivating and worthy subject to research. *Baldocchi et al.* [1991], *Rochette et al.* [1991], *Ehleringer and Field* [1993], and most recently *Irmak et al.* [2008] presented unique approaches of scaling-up r_s to r_c. The majority of these approaches, however, overlook the impact of atmospheric CO_2 levels on stomatal control of water loss from plant communities in the scaling-up process. Following up on a steady-state coupled water and carbon model developed by *Katul et al.* [2003], recently, *Katul et al.* [2009a] developed a stomatal optimization theory describing the effects of atmospheric CO_2 levels on leaf photosynthesis and transpiration rates that can be implemented in large-scale climate models. They showed that the cost of unit of water loss increases with atmospheric CO_2. Comparisons of their formulation results against gas exchange data collected in a pine forest showed that the formulation correctly predicted the condition under which CO_2-enriched atmosphere will cause increasing assimilation and decreasing g.

[6] In the scaling-up approach, each researcher scaled up r_s to r_c as a function of different microclimatological and/or physiological variables with successful applications. Nevertheless, difficulties and availability of r_c data for a variety of vegetation surfaces at different development stages and for a range of soil water and climatic conditions impose impediments to the practical application of the PM model to estimate evaporative losses from certain vegetation surfaces. Even if the r_s values of a given vegetation surface can be predicted with a reasonable accuracy, the challenge is still overcoming the added difficulties in the process of scaling up leaf level r_s to r_c to represent an integrated resistance from plant communities to quantify field-scale evaporative losses using the PM model [*Irmak et al.*, 2008]. Jarvis model estimates r_s, but r_c rather than r_s is needed as an input for the PM model. Any contributions to estimate r_c from more easily obtainable climatic variables, while maintaining the scientific merit and validity and robustness of the approach, can significantly augment the utilization of the Jarvis and PM models in practice by the water resource community. As an alternative to the physically based model scaling-up approach, an empirical approach is to estimate r_c from microclimatic observations. Our specific objectives with this research were to (1) develop a set of generalized-linear empirical models to estimate r_c as a function of

microclimatic variables for a nonstressed maize canopy, (2) investigate the relationships between primary microclimatic factors and r_c, and (3) present the practical implementation of the new models via experimental validation using scaled-up r_c data of porometer-measured leaf stomatal resistance data that were measured through an extensive field campaign in 2006. For further validation of the developed r_c models, we estimated actual evapotranspiration (E_{Ta}) for maize canopy on an hourly basis using modeled r_c from all models and compared the E_{Ta} estimates with the Bowen ratio energy balance system (BREBS)-measured E_{Ta} for an independent data set in 2005.

2. Materials and Methods

2.1. General Field Experimental Procedures

[7] Detailed descriptions of experimental procedures were presented by *Irmak and Mutiibwa* [2009], and only a brief description will be provided here. Extensive field data collection campaigns on r_s, leaf area index (LAI), plant height (h), and microclimatic variables, including incoming shortwave radiation (R_s), net radiation (R_n), leaf level photosynthetic photon flux density (PPFD), VPD, wind speed at 3 m (u_3), air temperature (T_a) at 2 m, relative humidity (RH) at 2 m, and other variables, were carried out in the summer of 2005 and 2006 at the South Central Agricultural Laboratory near Clay Center, Neb (latitude 40°34′N, longitude 98°08′W, and is 552 m mean sea level). Data were collected from a 13.5 ha maize (*Zea mays* L.) field irrigated with a subsurface drip irrigation system. Field maize hybrid Pioneer 33B51 with a comparative relative maturity of 113 to 114 days was planted at 0.76 m row spacing with a seeding rate of approximately 73,000 seeds ha^{-1} and planting depth of 0.05 m. Maize was planted on 22 April, emerged on 12 May, and reached full canopy closure on 4 July 2005. It reached silking stage on 12 July, matured on 7 September, and was harvested on 17 October in 2005. In 2006, maize was planted on 12 May with a planting density of 74,130 seeds ha^{-1}. Plants emerged on 20 May, reached complete canopy closure on 8 July, reached the silking stage on 15 July, started to mature on 13 September, and were harvested on 5 October 2006. The experimental field was irrigated two or three times a week to meet full plant water requirements. In 2005, total rainfall from 22 April to 30 September was 307 mm, and a total of 225 mm irrigation water was applied with the first irrigation starting on 30 June [69 days after planting (DAP)]. In 2006, total rainfall during the growing season (12 May to 30 September) was 362 mm, and a total of 172 mm of irrigation water was applied with the first irrigation starting on 16 June (35 DAP). The plant-available soil water in the effective plant rooting depth in the top 0.90 m soil layer was kept between near field capacity and the maximum allowable depletion to avoid plant water stress. Plants were fertilized based on soil samples taken prior to planting to determine the fertilizer needs with regular pest and disease control being undertaken when appropriate.

2.2. Evapotranspiration and Other Surface Energy Flux Measurements

[8] The surface energy balance components, including E_{Ta} and microclimatic variables were measured using a deluxe version of a Bowen ratio energy balance system (BREBS, Radiation and Energy Balance Systems, REBS, Inc., Bellevue, Wash) that was installed in the middle of the experimental field with a fetch distance of 520 m in the north-south direction and 280 m in the east-west direction. Net radiation was measured using a REBS Q*7.1 net radiometer that was installed approximately 4.5 m above the soil surface. Incoming and outgoing shortwave radiation envelopes were measured simultaneously using a REBS model THRDS7.1 (Radiation and Energy Balance Systems, REBS, Inc., Bellevue, Wash) double-sided total hemispherical radiometer that was sensitive to wavelengths from 0.25 to 60 μm. The chromel-constant and thermocouple for the T_a and RH probes (model THP04015 for T_a and THP04016 for RH; REBS, Inc., Bellevue, Wash), with a resolution of 0.0055°C for T_a and 0.033% for RH, were used to measure T_a and RH gradients. The BREBS used an automatic exchange mechanism that physically exchanged the T_a and RH sensors at two heights above the canopy. T_a and RH sensors were exchanged during the last 2 min of each 15 min interval. The left exchanger tube that houses the T_a and RH probes was in the lower position during the first and third 15 min periods of each hour, and the right tube was in the lower position during the second and fourth 15 min periods of each hour. Rainfall was recorded using a model TR-525 rainfall sensor (Texas Electronics, Inc., Dallas, Tex). Soil heat flux density (G) was measured using three REBS HFT-3.1 heat flux plates and three soil thermocouples. Each plate was placed at a depth of 0.06 m below the soil surface. The REBS STP-1 soil thermocouple probes were installed in close proximity to each plate at a depth of 0.06 m below the soil surface. Measured G values were adjusted to soil temperatures and soil water content as measured using three REBS SMP1R soil moisture probes. One soil moisture probe was installed in close proximity to each soil heat flux plate. Wind speed and direction at 3 m were monitored using a model 034B cup anemometer (Met One Instruments, Grant Pass, Ore). All variables were sampled every 60 s, averaged, and recorded every hour for energy balance calculations using a model CR10X datalogger and AM416 Relay Multiplexer (Campbell Scientific, Inc., Logan, Utah). The BREBS was closely supervised and general maintenance was provided at least once a week. Maintenance included cleaning the thermocouples and housing units (exchanger tubes), servicing radiometers by cleaning domes, checking/replacing the desiccant tubes, and making sure that the radiometers were properly leveled. The radiometer domes were replaced every 3–4 months. The lower exchanger tube was always kept at least about 1.0 m above the canopy throughout the growing season. The distance between the lower and upper exchanger tubes was kept at 0.90 m throughout the season [*Irmak et al.*, 2008; *Irmak and Mutiibwa*, 2008; *Irmak and Irmak*, 2008].

2.3. Stomatal Resistance and Plant Physiological Measurements

[9] A model AP4 dynamic diffusion porometer (Delta-T Devices, Ltd., Cambridge, UK) that was equipped with an unfiltered GaAsP photodiode light sensor with a spectral response similar to photosynthetically active radiation response was used to measure r_s on randomly selected green, healthy, and fully expanded leaves. Detailed description of number of r_s measurements, dates, and measurement protocols were presented by *Irmak et al.* [2008] and *Irmak and Mutiibwa* [2009]. Precautions were taken to maintain each leaf's natu-

ral orientation during the r_s measurements. Each reading corresponded to one complete diffusion cycle in which the sensor and leaf reached equilibrium with the RH. Readings were taken by orienting the position of the instrument user behind the plant and sunlight shadow (i.e., the plant leaves that were being measured were always between the instrument user and the sunlight) so that the shading of the sensors and the leaf was prevented. The readings were taken from the near-central portion of young and mature leaves. LAI was measured using a model LAI-2000 plant canopy analyzer (LI-COR Biosciences, Lincoln, Neb). Once a week, the field measurements were taken starting when LAI was about 1.2. On average, a total of 60 LAI measurements were taken on each measurement day and averaged for the day. Plant height was also measured from the soil surface to the tip of the tallest leaf from approximately 50 randomly selected plants.

2.4. Modeling Canopy Resistance

[10] Here we strategically evaluated the estimation of r_c from several directly measured environmental variables such as R_n, RH, T_a, u_3, and LAI. Readily available field-measurable variables (R_n, T_a, and RH) were given priority in modeling r_c by including them in all models developed. In addition, computed variables such as aerodynamic resistance (r_a), VPD, and solar zenith angle (Θ) were incorporated into the analysis to determine their role in the variation in r_c. Solar zenith angle was included with the hypothesis that it can help to capture temporal variability in r_c arising from the diurnal solar movement across the sky, such that as the sun moves across the horizon, there is a continuous redistribution of direct and diffuse sunlight in the canopy, subsequently affecting r_c. The r_a was evaluated with an expression that is derived from turbulent transfer and assuming a logarithmic wind profile [*Thom*, 1975; *Monteith and Unsworth*, 1990]. Following *Brutsaert and Stricker* [1979], we computed r_a (s m^{-1}) as

$$r_a = \frac{\ln\left[\frac{z_m - d}{z_{om}}\right] \ln\left[\frac{z_h - d}{z_{oh}}\right]}{k^2 u_z}, \quad (1)$$

where z_m is the height of wind measurements (3 m), z_h is the height of humidity measurements (2 m), d is the zero plane displacement height (m), z_{oh} is the roughness length governing transfer of heat and water vapor (m), z_{om} is the roughness length governing momentum transfer (m), k is von Karman's constant (0.41), and u_z is the wind speed at height z (3 m; m s^{-1}). We used measured plant height (h, m) to compute d, z_{om}, and z_{oh} following the study of *Monteith et al.* [1965], *Plate* [1971], and *Brutsaert* [1982]

$$d = 0.67h, \quad (2)$$

$$z_{om} = 0.123h, \quad (3)$$

$$z_{oh} = 0.10 z_{om}. \quad (4)$$

Since wind speed may induce temporary stomatal closure [*Salisbury and Ross*, 1992; *Kramer*, 1983], in addition to transfer of vapor and heat in the canopy, r_a may have an indirect effect on r_c. Thus, we incorporated u_3 into the models. Net radiation was included in all models because stomata generally do not respond to changes in the other environmental variables unless there is sufficient light for photosynthesis to occur [*Norman*, 1979; *Campbell*, 1982; *Massman and Kaufmann*, 1991; *Irmak et al.*, 2008].

[11] The observed r_c data used in this study as the reference r_c values to develop the models were scaled up from measured r_s values that were previously presented by *Irmak et al.* [2008] and *Irmak and Mutiibwa* [2009]. The modeling in this study is for empirically predicting r_c and not for scaling up r_s to r_c. *Irmak et al.* [2008] presented a methodology for scaling up r_s to r_c utilizing r_s versus a leaf level PPFD response curve that was measured through an extensive field campaign for a nonstressed maize canopy in 2006. *Irmak and Mutiibwa* [2008] measured r_s for subsurface drip-irrigated nonstressed maize plants and integrated a number of microclimatic and in-canopy radiation transfer parameters to scale up r_s to r_c. With the espousal of microclimatic and plant factors such as LAI for sunlit and shaded leaves, Θ, h, and direct and diffuse solar radiation, they scaled up r_s on an hourly basis as a main function of measured PPFD.

[12] The proposed r_c models of this study were developed using STATISTICA™ software (version 7.1, StatSoft, Inc., Tulsa, Okla) utilizing the generalized-linear/nonlinear model tool. The module is a comprehensive implementation of the general linear model. With this approach, both linear and nonlinear effects for any number and type of predictor variables (R_n, RH, u_3, T_a, VPD, LAI, r_a, and Θ) on a discrete or continuous dependent variable (r_c) can be analyzed [*McCullagh and Nelder*, 1989]. The generalized model is a generalization of the linear regression model, such that effects of climatic variables on r_c can be tested for categorical predictor variables, as well as for effects for continuous predictor variables. A categorical predictor variable is a variable, measured on a nominal scale, whose categories identify class or group membership, which is used to predict responses on one or more dependent variables. The general form of the generalized-linear equation we used was built upon Jarvis-type parameterization and relates a dependent variable (r_c) to a set of quantitative independent variables (R_n, RH, u_3, T_a, VPD, LAI, r_a, and Θ)

$$Y = b_0 + b_1X_1 + b_2X_2 + \ldots + b_kX_k + e, \quad (5)$$

where e is the error variability that cannot be accounted for by the predictors; note that the expected value of e is assumed to be zero, while the relationship in the generalized-linear model is assumed to be

$$Y = z(b_0 + b_1X_1 + b_2X_2 + \ldots + b_kX_k) + e, \quad (6)$$

where e is the error, and z (…) is a function. Formally, the inverse function of z(…), say f(…), is called the link function. The models were developed systematically and had a decreasing number of predictor variables from a maximum of eight predictors to a minimum of three. The form of the equations can be expressed as

$$r_{c\_1} = \exp(a + bR_n + cT_a + d\mathrm{VPD} + e\mathrm{RH} + fu_3 + gr_a + h\mathrm{LAI} + k\Theta), \quad (7)$$

$$r_{c\_2} = \exp(a + bR_n + cT_a + d\mathrm{VPD} + fu_3 + gr_a + h\mathrm{LAI} + k\Theta), \quad (8)$$

$$r_{c\_3} = \exp(a + bR_n + cT_a + e\mathrm{RH} + fu_3 + gr_a + h\mathrm{LAI} + k\Theta), \quad (9)$$

$$r_{c\_4} = \exp(a + bR_n + cT_a + e\mathrm{RH} + fu_3 + h\mathrm{LAI} + k\Theta), \quad (10)$$

$$r_{c\_5} = \exp(a + bR_n + cT_a + e\mathrm{RH} + fu_3 + h\mathrm{LAI}), \quad (11)$$

$$r_{c\_6} = \exp(a + bR_n + cT_a + e\mathrm{RH} + fu_3), \quad (12)$$

$$r_{c\_7} = \exp(a + bR_n + cT_a + e\mathrm{RH}), \quad (13)$$

where r_{c_i} is the canopy resistance estimated from model i (s m^{-1}), R_n is net radiation (W m^{-2}), T_a is air temperature (° C), RH is relative humidity (%), u_3 is wind speed measured at 3 m (s m^{-1}), r_a is aerodynamic resistance (m s^{-1}), LAI is green leaf area index, Θ is the solar zenith angle (degrees), a is the intercept, and b, c, d, e, f, g, h, and k are the coefficients of R_n, T_a, VPD, RH, u_3, r_a, LAI, and Θ, respectively, with all micrometeorological variables having hourly units.

2.5. Calibration and Validation of Proposed Canopy Resistance Models

[13] The scaled up hourly r_c data set used for calibration ranged from 19 June 2006 to 15 July 2006, and the data set for validation covered the period from 16 July 2006 to 31 August 2006. The coefficients of the models were optimized for the best fit of predicted values to observed values, i.e., maximizing the coefficient of determination (r^2) and minimizing the root mean square difference (RMSD) between measured and model-estimated r_c. In the calibration and validation, the r_c values that were observed from measured and scaled-up r_s values that were presented by *Irmak et al.* [2008] were used as the actual (reference) r_c values. These data sets were used to estimate (optimize) parameters for all seven r_c models. New parameters were estimated by searching over the parameter space to minimize the RMSD between observed (scaled-up) and model-estimated r_c. The optimized parameters replaced the original parameters and new r_c values were calculated for each model. The assumption we made in the model development was that there was no interaction effect of independent variables on r_c; thus, the variables act independently. All models were developed for an hourly time step using hourly input variables.

[14] Hourly r_c values computed from the seven models were compared to hourly r_c values (scaled up from measured r_s by *Irmak et al.*, 2008) for the 2006 growing season for validation. We further extended the validation of these models using the 2005 growing season. However, there was no measured r_s or scaled-up r_c data available in 2005. For further validation of our models in 2005, we estimated r_c values from the seven models from measured input variables to solve the PM model for hourly actual evapotranspiration (E_{Ta}) and compared the estimated E_{Ta} values with the BREBS-measured E_{Ta}. The form of the PM equation we used is

$$\lambda E_{Ta} = \frac{\Delta(R_n - G) + \rho c_p \frac{e_s - e_a}{r_a}}{\Delta + \gamma\left(1 + \frac{r_c}{r_a}\right)}, \quad (14)$$

where λE_{Ta} is the latent heat flux density (W m^{-2}), G is the soil heat flux density (W m^{-2}), Δ is the slope of the saturation vapor pressure and air temperature curve (Pa °C^{-1}), ρ is the air density (kg m^{-3}), c_p is the specific heat of air (J kg^{-1} °C^{-1}), γ is the psychometric constant (Pa °C^{-1}), e_s and e_a, respectively, are the saturation and actual vapor pressure of air (Pa) where $e_s - e_a$ represents VPD, and R_n is the net radiation (W m^{-2}).

2.6. Statistical Analyses

[15] The ability of the proposed r_c models to predict the resistances was analyzed using three statistics. The r^2 was used as a measure of goodness of fit (i.e., the measure of total variance accounted for by the model). The RMSD was used as a measure of the total difference between the predicted and observed r_c values. We used modeling efficiency (EF) to asses the fraction of the variance of the observed values which is explained by the model, so EF provides good measure of model performance. In the EF, the higher values indicate better agreement and the best model is the one with a value of EF closest to unity. Physically, EF is the ratio of the mean square error to the variance in the observed data and subtracted from unity. The EF is an improvement in model evaluation in that it is sensitive to differences in the observed and model-simulated means and variances. However, because of the squared differences, EF can be overly sensitive to extreme values. The EF is expressed as

$$\mathrm{EF} = 1 - \frac{\sum (O_i - P_i)^2}{\sum (O_i - \overline{O})^2}, \quad (15)$$

where O_i and P_i are the observed and predicted r_c values, respectively, and $\overline{O}$ is the mean of observed data. All statistical analyses were performed using STATISTICA™ (ver. 7.1, StatSoft, Inc., Tulsa, Okla).

3. Result and Discussion

3.1. Climatic Conditions

[16] A summary of the measured meteorological data for the 2005 and 2006 growing seasons and long-term (32 year) average values are presented in Table 1. During 2006, the year used for model calibration, rainfall from April through July (245 mm) was less than the long-term average (374 mm). August was wetter than average (119 mm versus 83 mm), and daily average incoming shortwave solar radiation (R_s) was less (224 W m^{-2}) as compared with the previous 4 months of the growing season. Maximum T_a was 1.5 to 3.5°C higher than the long-term average from May to July. Similarly, R_s was 18 to 31 W m^{-2} greater than the long-term average in the same time period. Relative humidity was also less in 2006 than in an average year. Average wind speed was very similar to long-term average values. From March to August 2006, the T_{a_min} was, on average, 1.3°C higher than the long-term average. Overall, 2006 was warmer and drier than an average year. Year 2005, which was used for model validation, was drier than a normal year with 72% normal total rainfall. On a seasonal average T_{a_max} in 2005 was 0.6°C higher than the average with T_{a_max} in September averaging 2.2°C higher than the average. The warmest month was July with an average T_{a_max} of 30.4°C. The seasonal average T_{a_min} was 1.4°C higher, and R_s was 14 W m^{-2} higher than the average.

Table 1. Meteorological Parameters Measured for the Period of March–October at Clay Center, Neb[a]

Period	Meteorological Variable	March	April	May	June	July	August	September	October
2005	u_3 (m s^{-1})	4.7	5.1	5.0	3.7	2.4	1.7	2.4	3.1
	T_{a_max} (°C)	11.6	17.3	23.3	28.4	30.4	27.8	27.5	19.4
	T_{a_min} (°C)	−1.9	4.5	9.6	16.5	17.8	16.7	13.4	5.7
	RH_{avg} (%)	66.8	68.5	63.6	71.2	70.7	78.3	68.2	67.2
	R_s (W m^{-2})	150.4	206.5	259.0	279.3	283.0	223.1	207.8	145.6
	R_n (W m^{-2})	71.0	108.5	138.7	172.1	174.4	132.8	111.2	59.2
	Rainfall (mm)	52.4	64.4	41.7	77.1	69.6	60.4	42.6	32.2
2006	u_3 (m s^{-1})	4.6	4.9	4.7	3.2	1.7	1.5	1.9	3.4
	T_{a_max} (°C)	9.1	20.5	24.3	29.6	30.3	27.8	22.9	16.1
	T_{a_min} (°C)	−2.7	5.2	10.8	15.9	18.3	17.0	9.7	3.4
	RH_{avg} (%)	72.7	64.6	61.0	65.2	73.4	79.8	71.3	70.3
	R_s (W m^{-2})	157.6	214.0	256.3	288.4	278.4	224.8	181.8	120.4
	R_n (W m^{-2})	72.0	111.4	141.8	169.5	174.0	142.1	108.5	53.8
	Rainfall (mm)	4.3	46.5	60.1	54.2	83.8	118.9	75.9	21.8
Long-term average (1975–2007)	u_3 (m s^{-1})	4.1	4.4	4.0	3.5	2.9	2.6	3.1	3.3
	T_{a_max} (°C)	10.5	17.0	22.5	28.1	30.3	29.2	25.3	18.3
	T_{a_min} (°C)	−3.2	2.4	9.3	14.6	17.3	16.3	10.7	3.6
	RH_{avg} (%)	69.8	66.3	71.3	70.2	73.2	74.5	68.8	67.2
	R_s (W m^{-2})	156.6	196.0	225.0	259.8	259.8	228.5	184.4	131.1
	Rainfall (mm)	40.0	59.0	112.0	110.0	93.0	83.0	63.0	45.0

[a]Wind speed at 3 m (u_3), maximum and minimum air temperature (T_{a_max} and T_{a_min}), average relative humidity (RH_{avg}), average incoming shortwave radiation (R_s), average net radiation (R_n), and total rainfall.

Wind speed and relative humidity values were similar to the long-term average values.

3.2. Seasonal Patterns of Hourly Canopy and Aerodynamic Resistances

[17] Hourly r_c decreased from early season during partial canopy toward midseason in early July, remained relatively stable until mid-August, and increased again, slightly, until late August (Figure 1a). Similar to other studies [*Monteith*, 1995; *Alves et al.*, 1998; *Perez et al.*, 2006], we observed a typical theoretically expected parabolic variation in the diurnal trend of r_c in Figure 1a, characterized by a high resistance in the morning, gradually decreasing to a minimum in between 13:00 and 16:00 pm and gradually increasing in the afternoon until sunset. The profile of the graph is explained by the soil-plant-atmosphere continuum such that as long as the soil profile can supply the water to meet the evaporative atmospheric demand, r_c will decrease with increasing radiation. However, when the evaporative demand exceeds the rate of soil water absorption at the root zone, typically in the afternoon, r_c may increase to reduce transpiration.

[18] From 19 June until first week of July, r_c was at its greatest values ranging from a daily minimum of 50–60 s m^{-1} to around 200 s m^{-1}. The r_c and LAI showed an inverse relationship, where r_c decreased as LAI increased. r_c remained relatively stable when LAI reached 3.5–4.0. The maximum r_c occurred on 24 June at 09:00 am as 216 s m^{-1}. During that hour, the following conditions were observed: LAI = 1.6, u_3 = 3.3 m s^{-1}, T_a = 17.9°C, RH = 93.9%, R_s = 109.3 W m^{-1}, and R_n = 57.4 W m^{-2}, with a moderate atmospheric demand (VPD = 0.80 kPa). This high r_c value (216 s m^{-1}) can also be a result of dew formation on the leaves. On average, r_c fluctuated within a magnitude of about 50 s m^{-1} diurnally. Diurnal fluctuations were greatest (>70–75 s m^{-1}) early in the season and least (≈30 s m^{-1}) in the midseason. The maximum diurnal fluctuation range of r_c was observed on 24 June as 140 s m^{-1}. r_a followed a similar trend as r_c throughout the season with lower magnitudes (Figure 1a). r_a was also high during the early season when plant was short, gradually decreased toward midseason, and slightly increased again after mid-August. r_a ranged from approximately 3 s m^{-1} in midseason to around 60 s m^{-1} in early season. The maximum r_a was obtained on 25 June as 67.7 s m^{-1} when h = 1.8 m, LAI = 1.57, and within a daily average r_c = 98.3 s m^{-1}. r_a remained relatively constant during the mid season due to constant h (ranging between 2 and 2.2 m), fluctuating in a narrow range between 10 to 20 s m^{-1}. The seasonal average r_a was 15.9 s m^{-1}.

3.3. Relationship Between r_c and Micrometeorological Variables

[19] The relationships between r_c versus T_a, RH, VPD, R_n, R_s, u_3, wind direction, LAI, Θ, and r_a on an hourly basis are presented in Figures 2a–2j, respectively. We used linear regression, exponential, or power functions as the best-fit functions, depending on the distribution of the data. The relationships between r_c versus u_3, wind direction, and Θ were weak. There was a strong relationship between r_c and T_a, and the T_a range during the season was between 15.7°C to 39°C (Figure 2a). We found larger values and a larger range of values of r_c for T_a values <29°C. r_c responded to T_a in a much narrower range for temperatures >29°C. Although there was a general trend of increasing r_c with increasing RH, this relationship is not strong (r^2 = 0.12, Figure 2b). The response of r_c to VPD was stronger than to RH with r^2 = 0.23. *Aphalo and Jarvis* [1991] investigated the response of stomata to leaf surface humidity and temperature and showed that the relationship between g and RH was different when measured at the same temperature rather than at different temperatures. They observed a reversible response to RH under constant temperature and that there was also a response to temperature under constant RH. An inversely proportional response was consistently obtained when g was expressed in relation to VPD. *Mott and Parkhurst* [1991] and *Oren et al.* [1999] showed that the response of stomata is not to VPD (or RH) directly, but it is the transpiration rate which responds directly to VPD. However, this may not be the only mecha-

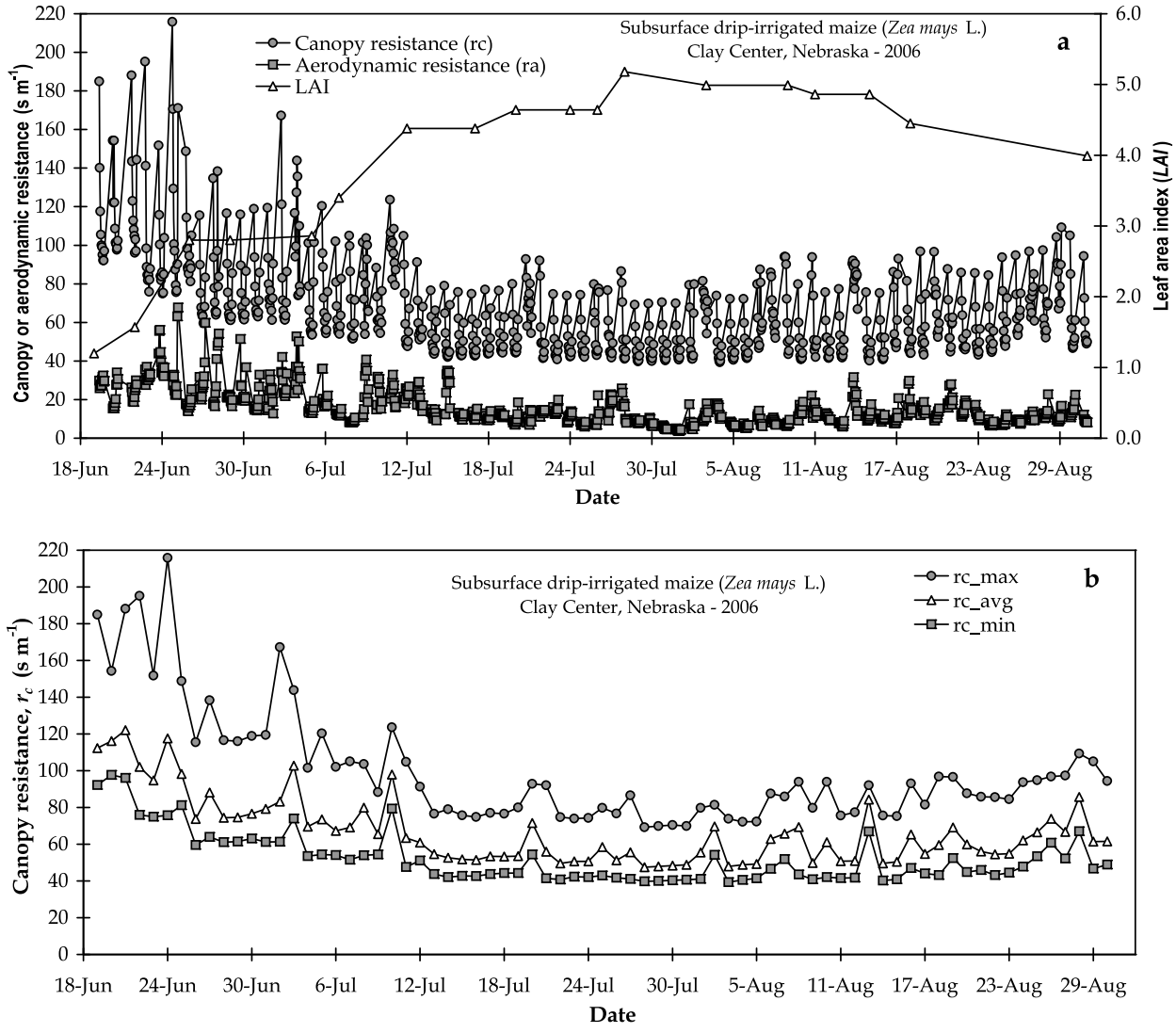

Figure 1. (a) Seasonal pattern of hourly canopy resistance (r_c) and aerodynamic resistance (r_a) in relation to leaf area index (LAI), and (b) and seasonal daily pattern of maximum, average, and minimum canopy resistance for a nonstressed maize canopy.

nism that causes changes in r_s. Other factors such as change in leaf water potential as a result of transpiration responding to VPD is most likely responsible for changes in r_s due to this signal (respond to change in water potential) transferring to the guards cells. A number of leaf-level semi-empirical models used different forms of functions of either RH or VPD when modeling stomatal response. For example, the models proposed by *Ball et al.* [1987] (Ball-Berry model) and *Collatz et al.* [1991] suggest that g is somewhat linear in RH. Others semiempirical in VPD (based on *Leuning et al.* [1995]) and a new class of models based on optimization theories suggest a $VPD^{0.5}$ dependence of g (i.e., a power-law versus exponential). Another study showed a log(VPD) dependence of g [*Oren et al.*, 1999]. *Oren et al.* [1999] also showed that stomatal sensitivity is proportional to the magnitude of g at low VPD ($\leq$1 kPa) and concluded that plant species with high g at low VPD show a greater sensitivity to VPD. The linear model presented by *Katul et al.* [2009b] is consistent with aforementioned studies in terms of the dependency of g to VPD. The main rationale of using RH rather than VPD in our models will be discussed in section 3.4.

[20] As expected, the response of r_c to R_n was much stronger than for R_s (Figures 2d and 2e) (r^2 = 0.34 for R_n versus r^2 = 0.10 for R_s), since R_n, rather than R_s, represents the amount of energy intercepted at the canopy level that cause a response in stomata. Higher r_c values were observed at lower R_n values due to the larger magnitude of stomatal closure at lower R_n even when other environmental factors change. The maximum r_c (216 s m^{-1}) occurred at R_n = 0.33 MJ m^{-2} h^{-1}, and the minimum usually occurred when R_n was greater than 2 MJ m^{-2} h^{-1}. There were many hours when r_c did not respond to changes in R_n due to the control of r_c by other microclimatological variables. Even though there is enough R_n, high u_3, low VPD, small LAI, and low T_a will have an impact in controlling the opening or closure of stomata. Stomatal response to both R_n and R_s was discussed in detail by *Irmak and Mutiibwa* [2009]. We observed several different groupings of r_c with R_n in Figure 2d

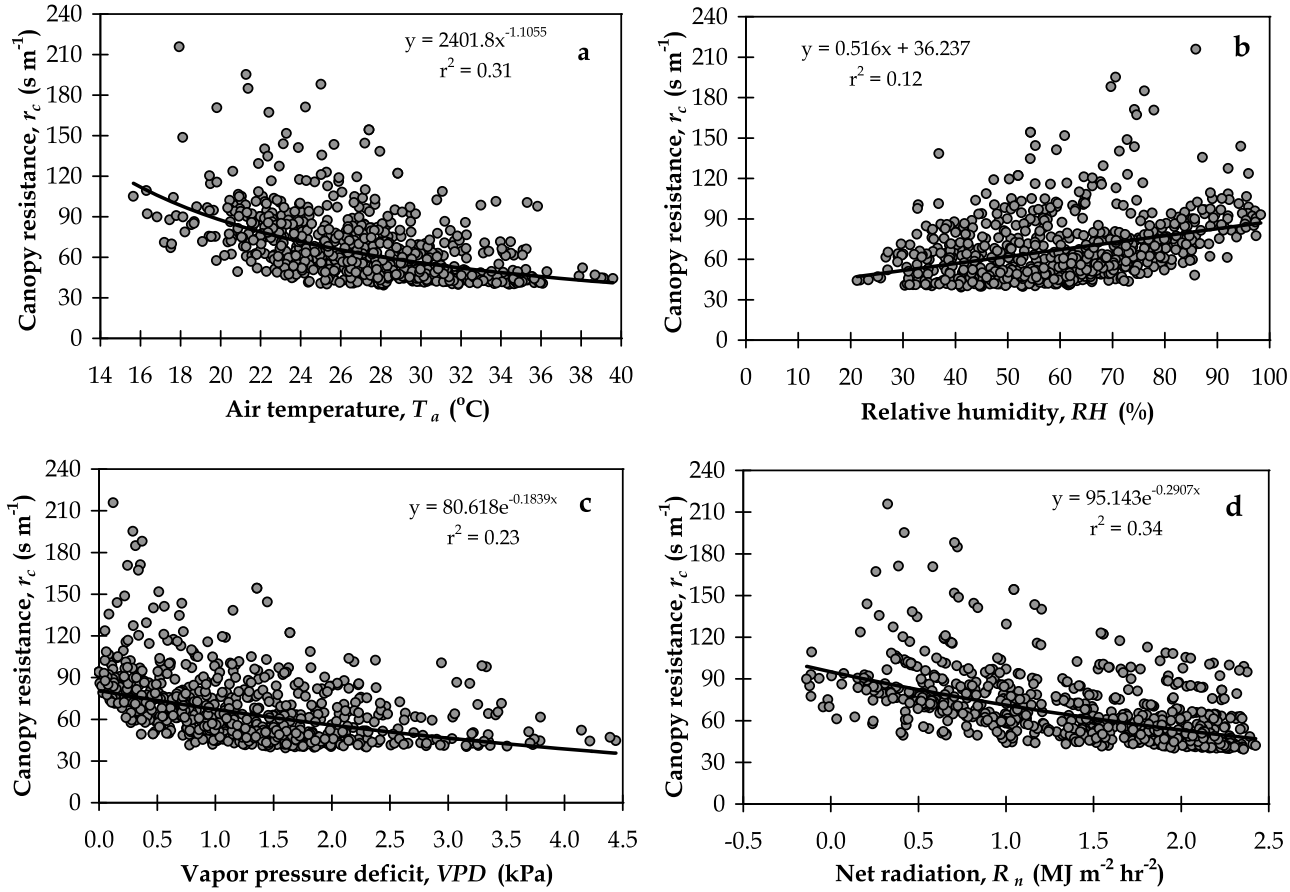

Figure 2. Relationship between canopy resistance (r_c) and primary microclimatic variables: (a) air temperature (T_a), (b) relative humidity (RH), (c) vapor pressure deficit (VPD), (d) net radiation (R_n), (e) incoming shortwave radiation (R_s), and (f) wind speed at 3 m (u_3) (n = 755 for each case). Relationship between canopy resistance (r_c) and main microclimatic variables: (g) wind direction, (h) leaf area index (LAI), (i) solar zenith angle (Θ), and (j) aerodynamic resistance (r_a) (n = 755 for each case).

that does not occur as much with R_s in Figure 2e. The reason for this fluctuation or groupings is not clear to the authors. While the relationship between r_c and u_3 is not very clear, there was a tendency of increasing r_c with increasing u_3. The highest r_c values were obtained in the u_3 range of 2 to 4 m s^{-1} (Figure 2f). As observed by *Monteith et al.* [1965], there is slight evidence in Figure 2f that the r_c responds to u_3 at higher wind speeds, but the changes in r_c are too small.

[21] Figure 2h presents the relationship between daily LAI and hourly r_c. The relationship between the r_c and LAI is the strongest among all variables (r^2 = 0.41). r_c decreased gradually as LAI increased from 1.20 to 5.30. The magnitude of diurnal fluctuation in r_c was greater in the early season than in the middle and late season. The larger variations in r_c at lower LAI and partial canopy cover early in the season were caused by the dry soil surface and higher soil evaporation. The inverse relationship between LAI and r_c did not hold after approximately LAI = 4.0, although diurnal fluctuation in r_c was still present. Both variables remained relatively stable for the rest of the season. While the impact of soil surface evaporation on r_c is not fully understood, r_c usually increases as soil water is depleted. *Ham and Heilman* [1991] showed that the within-canopy aerodynamic and soil resistance to water vapor transport from the soil surface were greater than those for the canopy even at low wind speeds. Although *Tanner* [1963] suggested that r_c contains an aerodynamic component depending on wind speed, our findings support the suggestion of *Monteith et al.* [1965] that resistance is governed primarily by LAI (Figure 2h), light (Figure 2d), temperature (Figure 2a), and VPD (Figure 2c) and is independent of the intensity of turbulent mixing above or within the canopy. This may suggest a high canopy coupling (omega factor, Ω) [*McNaughton and Jarvis*, 1983; *Jarvis and McNaughton*, 1986] between canopy and microclimate above the canopy surface. While quantification of Ω was beyond the scope of this study, it is a powerful parameter that describes how strongly the VPD at the canopy surface is linked the boundary layer above the canopy and examines the contribution of radiation and VPD to the transpiration rate [*Jarvis and McNaughton*, 1986].

[22] The relationship between r_c and r_a is presented in Figure 2j. The deviation between both resistances is smaller in the low resistance range, while r_c is always larger than r_a. On a seasonal average, r_c was 3.5 times larger than r_a. It is expected that r_a would be smaller than r_c because the evaporative loss is mainly controlled by r_c. Thus, higher resistance exists at the canopy level for vapor transport. Also, r_a is often the dominant mechanism for the absorption

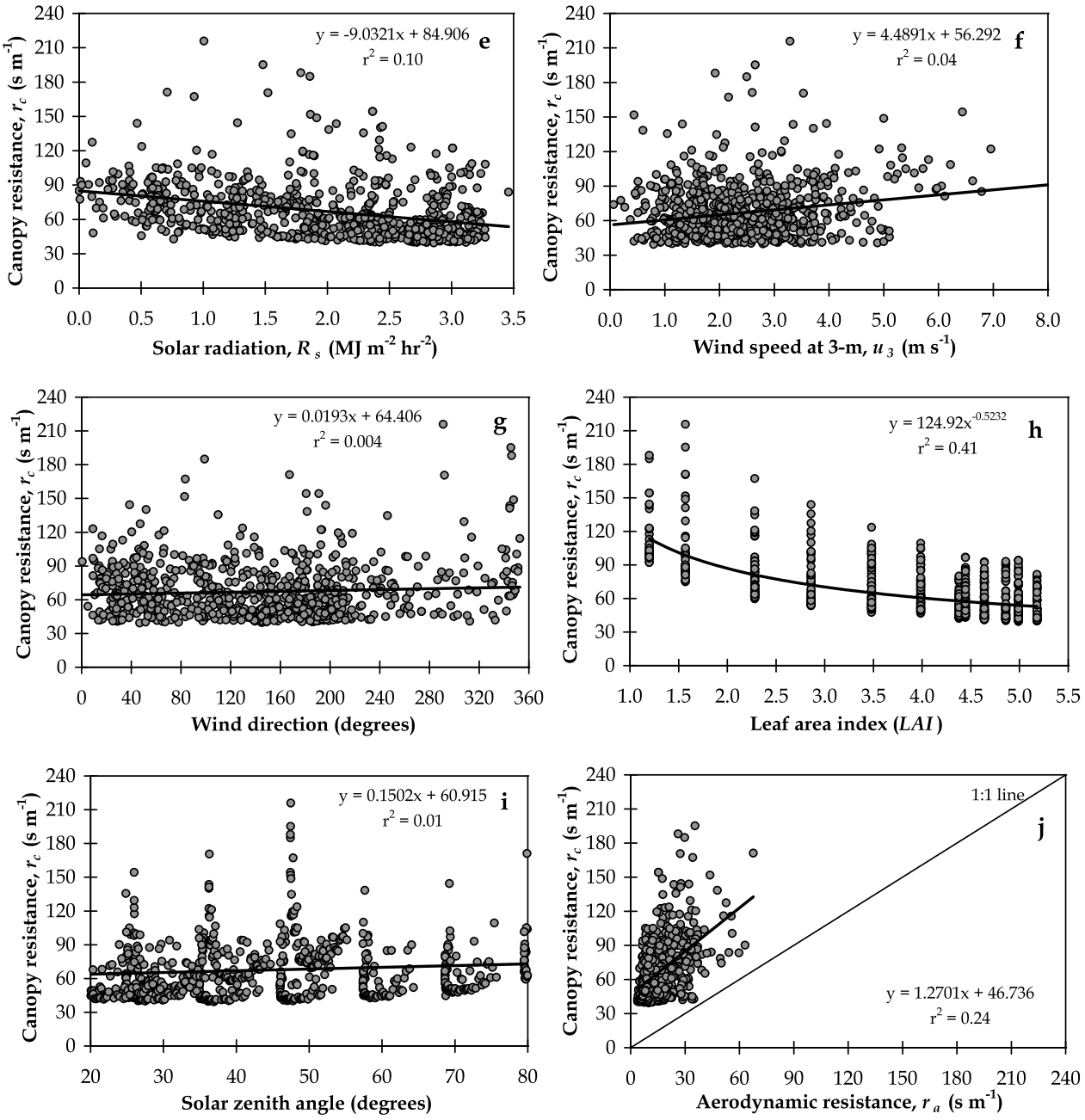

Figure 2. (continued)

of momentum by vegetation so that the resistance to the exchange of momentum between the canopy and surrounding air is smaller than the corresponding resistances to the exchange of heat and vapor, which depend on molecular diffusion alone [*Monteith and Unsworth*, 1990]. *Monteith and Unsworth* [1990] analyzed the ratio r_c/r_a for several mature forest sites and found that the ratio r_c/r_a is about 50. The ratio can be used as an indicator of the evaporative ratio from wet versus dry canopies. They stated that larger ratios of r_c/r_a (e.g., 50) would show that evaporation from forest canopies wet with rain would proceed much faster than from dry canopies exposed to the same microclimatic conditions. Consequently, forests in regions where rain is frequent tend to use more water by evaporation from foliage and transpiration than shorter plants growing nearby. They reported that this contrasts with the situation for many agricultural plants, such as maize, for which minimum values of r_c are typically 100 s m^{-1} but r_c/r_a is often close to unity. In our case, the minimum r_c ranged from 40 to 100 s m^{-1} (Figure 1b). We found that the hourly r_c/r_a ratios for our experimental conditions ranged from 1.2 to 14 (Figure 3) with a seasonal average ratio of 5.1, which is much lower than the forest

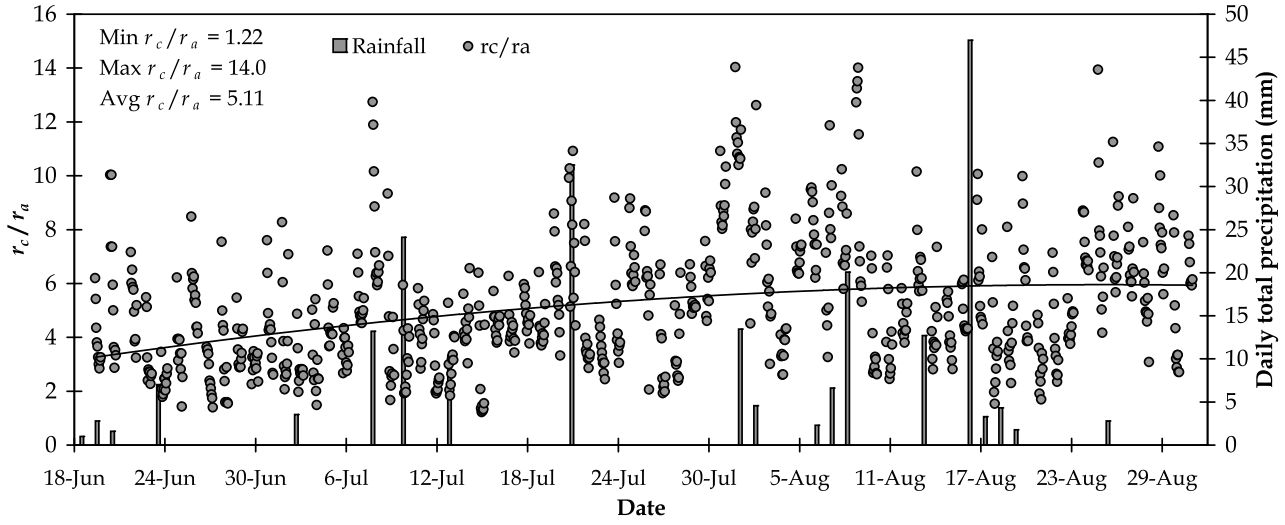

Figure 3. Hourly ratios of canopy resistance (r_c) to aerodynamic resistance (r_a) (r_c/r_a) in relation to precipitation for a nonstressed maize canopy.

canopy as reported by *Monteith and Unsworth* [1990]. Although we did not observe a distinct pattern in the ratio throughout the season, it was lower early in the season, ranging from 1.0 to 8.0; greater in the midseason, fluctuating between 2 and 14, and remained relatively stable around 6.0 from mid-August to the end of the season, although fluctuations were still present. In general, we found that the r_c/r_a ratio tended to decrease sharply after rain events.

3.4. Canopy Resistance Model Calibration and Validation Results

[23] The calibration coefficients *b*, *c*, *d*, *e*, *f*, *g*, *h*, and *k* and the intercepts (*a*) for the 2006 growing season for the seven models (equations 7–13) are presented in Table 2. Model calibration performance results are presented in Figures 4a–4g. Models r_{c_1}, r_{c_2}, r_{c_3}, and r_{c_4} had very similar r^2 (~0.95) and RMSD (~5.0 s m^{-1}). Model r_{c_1} had the highest number of modeling variables (R_n, T_a, VPD, RH, u_3, r_a, LAI, and Θ). Models r_{c_6} and r_{c_7} had very similar performance and had the poorest r^2 of 0.44 and highest RMSD of 17.4 s m^{-1}. These two models had the least number of modeling variables, r_{c_6} with 4 variables (R_n, T_a, RH, and u_3) and r_{c_7} with 3 variables (R_n, T_a, and RH). The model r_{c_5} had a good r^2 of 0.93 and low RMSD of 6.3 s m^{-1}. The observed seasonal mean r_c was 75 s m^{-1}, and the means from all seven models were very similar to the observed value. Estimates from the first five models were very good with very little scatter in the data around the 1:1 line. Models r_{c_6} and r_{c_7} overestimated in the range of 0 to around 90 s m^{-1} and underestimated at greater values. The data scatter increased for both models in the higher r_c range. The coefficients for T_a and RH for models r_{c_6} and r_{c_7} are different than other models, whereas the coefficients for other variables were similar for most models. The variation in coefficients for T_a and RH for models r_{c_6} and r_{c_7} may be due to exclusion of LAI from these two models such that the influence of T_a and RH on r_c was different than other models in the absence of LAI in estimating r_c.

[24] The seasonal distribution of the hourly residuals that were calculated from the regression between the model estimates of r_c (r_{c_1} through r_{c_7}) versus observed r_c for the calibration data set are presented in Figure 5. Models r_{c_1} though r_{c_5} had lower residuals than the models r_{c_6} and r_{c_7}. The residuals for the models r_{c_1} through r_{c_5} showed similar trends and tend to fluctuate between similar ranges of −20 to 20 s m^{-1}. The residuals were higher early in the growing season and fluctuated in a narrower range towards the end of the season. Models r_{c_6} and r_{c_7} had larger residual fluctuations ranging from −35 to 65 s m^{-1}.The residuals for these two models were high early in the season, gradually decreased toward the midseason, and remained negative from early July to the end of July. Model r_{c_1} had the lowest and models r_{c_6} and r_{c_7} had the largest residuals. Overall, the sum of squares of the residuals were 8470, 9331, 8649, 8768, 12,754, 45,345, and 45,472 for the models r_{c_1} through r_{c_7}, respectively. The mean squares of the residuals were 24.8, 27.7, 25.7, 26, 37.8, 134.6, and 135 for the same models, respectively. Except LAI, we did not observe any clear trend of the residuals with respect to any of the micrometeorological drivers measured.

3.5. Validation of r_c Models for Estimating Observed r_c in 2006

[25] We validated the models in two ways. First, the models were used to estimate r_c from 21 July to 30 August in 2006 growing season and the validation results are presented in Figure 6. Compared to the calibration results, the validation RMSD values increased by about 5 s m^{-1} for all models, and the r^2 decreased to a range of 0.69 to 0.73. The r^2 of 0.71 and 0.70 was a significant improvement in performance for models r_{c_6} and r_{c_7}, which had a calibration r^2 of 0.44. Models r_{c_1}, r_{c_2}, r_{c_3}, r_{c_4}, and r_{c_5} had means ranging from 50.3 to 51.5 s m^{-1}, which was close to the observed mean (55.9 s m^{-1}). The means of r_{c_6}, and r_{c_7} were 76.1 and 75.9 s m^{-1}. With the EF ranging from 0.57 to 0.65, models r_{c_1}, r_{c_2}, r_{c_3}, r_{c_4}, and r_{c_5} demonstrated a

Table 2. Calibration Coefficients[a] for the Seven Models Developed to Predict Canopy Resistance as a Function of Net Radiation, Air Temperature, Vapor Pressure Deficit, Relative Humidity, Wind Speed at 3 m, Aerodynamic Resistance, Leaf Area Index, and Solar Zenith Angle

Coefficient	Variable	Models and Coefficients						
		r_{c_1}	r_{c_2}	r_{c_3}	r_{c_4}	r_{c_5}	r_{c_6}	r_{c_7}
	Mean r_c	74.9	74.8	74.9	74.9	74.9	75.0	75.0
a	Intercept	5.12	5.31	5.17	5.27	5.07	5.59	5.67
b	R_n	−0.39	−0.40	−0.39	−0.40	−0.34	−0.19	−0.20
c	T_a	0.01	0.01	0.01	0.01	0.0035	−0.03	−0.03
d	VPD	−0.04	−0.09	-	-	-	-	-
e	RH	0.0027	-	0.00357	0.00344	0.0046	−0.00207	−0.0025
f	u_3	0.03	0.03	0.03	0.02	0.03	0.01	-
g	r_a	0.0016	0.0016	0.0012	-	-	-	-
h	LAI	−0.24	−0.24	−0.24	−0.25	−0.24	-	-
k	Θ	−0.0023	−0.0022	−0.0027	−0.00277	-	-	-

[a] a, b, c, d, e, f, g, h, and k; measured mean r_c was 75 s m^{-1}.

high efficiency since values of EF close to 1 signify a good modeling performance. Although the RMSD and r^2 results of models r_{c_6}, and r_{c_7} were acceptable, the EF values were −1.096 and −1.087, respectively. A negative EF indicates that the squared difference between the model predictions and the observed values is larger than the variability in the observed data. Thus, the observed mean is a better predictor than the model. The poor EF of models r_{c_6} and r_{c_7} was further depicted by the slopes, which showed an overestimation of 33% by both models (Figure 6). Model r_{c_6} is different from r_{c_7} because of the inclusion of u_3; however, from the statistical results in Table 2, the two models presented similar performance. It appears that the performance of models r_{c_6} and r_{c_7} was compromised by using fewer variables that influence r_c.

[26] Overall, model r_{c_5} performance had the best agreement with the data. The model had the smallest RMSD of 9.3 s m^{-1}, highest r^2 of 0.73, the highest EF of 0.65 with only 6% underestimation. Model r_{c_5} has 5 variables (R_n, T_a, RH, u_3, and LAI) with the latter being the only variable not measured by a typical weather station. This is an encouraging performance of the model using readily available weather station data. LAI has been used in both single and multiple layered models as a weighting or scaling factor of r_s to estimate r_c [*Szeicz and Long*, 1969; *Sinclair et al.*, 1976; *Whitehead and Jarvis*, 1981; *Bailey and Davies*, 1981; *Seller et al.*, 1986]. Similar to the results presented by *Beadle et al.* [1985], we observed that the r_c is considerably influenced by seasonal changes in LAI, and we demonstrated the negative impact of exclusion of LAI, the only plant physiological variable, on r_c in the performance of models r_{c_6}, and r_{c_7}, where performance statistics were poor compared to the other models that included LAI.

[27] The performance of model r_{c_1}, which used eight variables, was not different from models r_{c_2}, r_{c_3}, r_{c_4}, and r_{c_5}, which used 5 to 7 variables. To select the better variable between VPD and RH for modeling r_c, models r_{c_2} and r_{c_3} were developed with the same number of variables but with one, model r_{c_2}, using VPD and the model r_{c_3}, using RH. Clearly, the results in Figure 6b versus 6c suggest that RH was a better predictor than VPD with a smaller RMSD and greater r^2 and EF. In model r_{c_3}, using RH instead of VPD resulted in 4%, 6%, and 8% improvement in r^2, RMSD, and EF, respectively. However, the residuals for model r_{c_2} and r_{c_3} were similar in magnitude and distribution and the improvement in predicted r_c using r_{c_3} was not statistically significant ($P > 0.05$) than predictions of r_{c_2}. Nevertheless, since the objective of the study was to model r_c from weather station-measured climate variables, this was an important finding, and as such, RH rather than VPD was used as a variable for the rest of the models (r_{c_3}, r_{c_4}, r_{c_5}, r_{c_6}, and r_{c_7}).

[28] *Baldocchi et al.* [1991], *Finnigan and Raupach* [1987], *Alves et al.* [1998], and *Alves and Pereira* [2000] have pointed out that r_c contains additional nonphysiological information pertaining to the r_a in the canopy. Therefore, model r_{c_3} was set up to be different from model r_{c_4} by the inclusion of r_a. However, similar to the results obtained by *Finnigan and Raupach* [1987], the results (r^2 and EF) in Figures 6c and 6d showed that r_a added a minimal improvement in estimating r_c. Conversely, elimination of Θ as an independent variable from the model r_{c_5} resulted in an improvement in RMSD, r^2, and EF. This suggests that r_a and Θ are of minimal importance in the modeling of r_c. The results demonstrate that models like r_{c_5}, with the variables R_n, RH, T_a, u_3, and LAI rather than including all variables, such as in model r_{c_1}, can provide good performance. This might be due to the fact that inclusion of many independent variables in r_c modeling can also increase the variability, error, and uncertainty associated with obtaining those variables, thus, negatively impacting the model performance. On the other hand, enough independent variables must be accounted for when modeling r_c and our results indicated that the model r_{c_5} seems to represent this balance (number of variables versus performance).

[29] Figures 6a–6g show a cluster of points of small r_c values which gradually spread out and decrease in number with increasing variability as the resistances increase. This shows that for a well-watered field, r_c is dominated by small resistance values, with a few high resistance values generally observed in the morning, late afternoon, and during advection and extreme conditions. In comparison to the 1:1 line, the graphs show that models r_{c_1}, r_{c_2}, r_{c_3}, r_{c_4}, and r_{c_5} underestimated resistance, whereas r_{c_6} and r_{c_7} overestimated observed r_c. Models, r_{c_1}, r_{c_2}, r_{c_3}, r_{c_4}, and r_{c_5} underestimated observed r_c by 8%, 10%, 8%, 8%, and 6%, respectively. Both r_{c_6} and r_{c_7} overestimated by 33%. In Figures 6a–6g, we observed an increase in variability with increasing r_c for all models. Increased variability could be associated with the rigidity of the models to adjust and depict the limiting variables during extreme conditions. For instance, in the morning hours, R_n is the limiting factor of r_c.

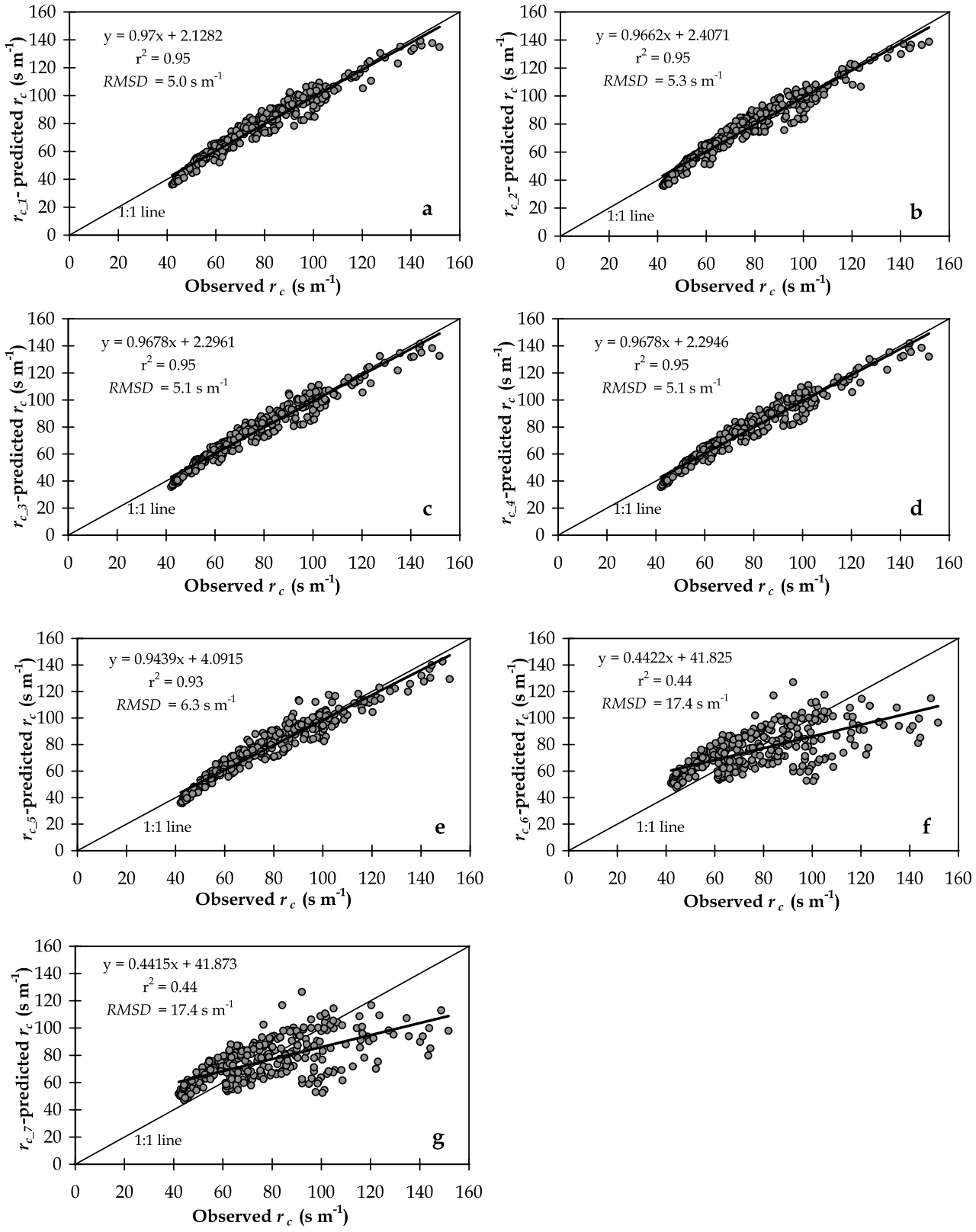

Figure 4. Calibration (19 June to 15 July 15) performance results for the seven canopy resistance (r_c) models (n = 405 for each case).

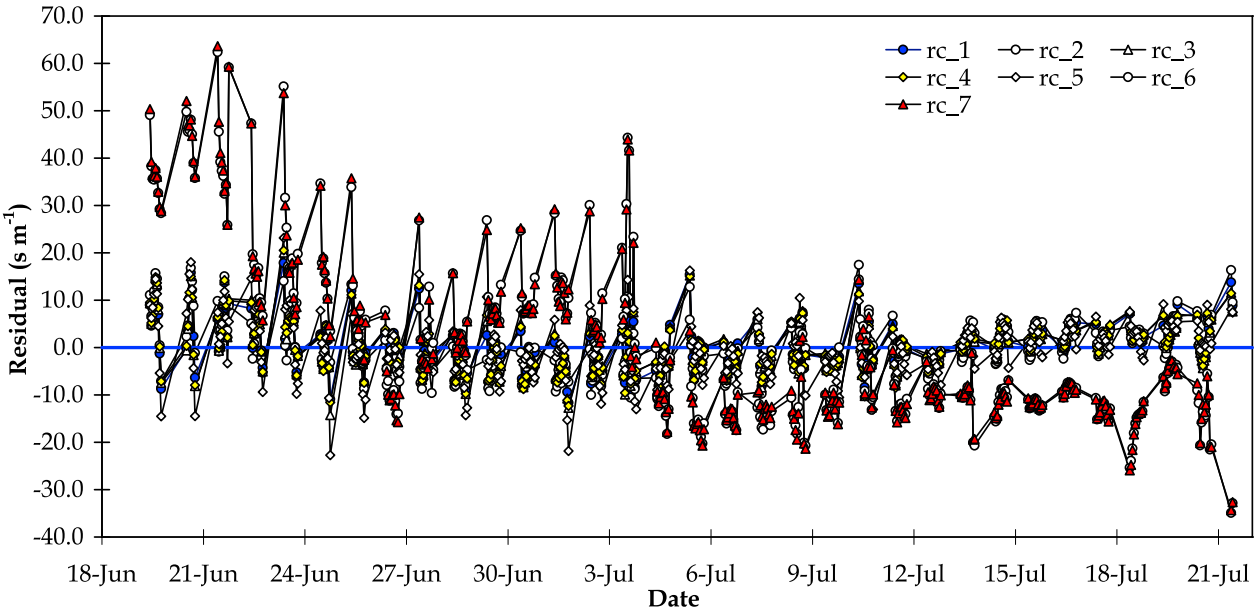

Figure 5. Distribution of residuals of regression between modeled canopy resistance (r_{c_1} through r_{c_7}) and observed r_c for the growing season (19 June to 15 July 2006) for the calibration data set (n = 339).

In the afternoon, studies [*Adams et al.*, 1991] have shown that VPD, which is regulated by RH, is typically the limiting factor.

3.6. Validation of r_c Models for Estimating E_{Ta} in 2005

[30] Further validation of r_c model performance was done on an independent data set by estimating r_c from each model on an hourly basis and then using the PM model as a one-step procedure to estimate E_{Ta} from modeled r_c. We then compared the PM-estimated E_{Ta} to the BREBS-measured E_{Ta} on an hourly basis. The seasonal distribution of hourly BREBS-measured E_{Ta} data from 1 May to 31 August that were used is presented in Figure 7. Hourly E_{Ta} ranged from near zero to 1.16 mm h^{-1}. There was a strong agreement between the BREBS-measured and the PM-estimated E_{Ta} (Figure 8a–8g for models r_{c_1} through r_{c_7}, respectively). The results show that the performance of all models is similar with r^2 ranging from 0.88 to 0.90. The RMSD ranged from 0.09 mm h^{-1} for models r_{c_6} and r_{c_7} to 0.13 to 0.15 mm h^{-1} for other models. The E_{Ta} estimated with r_c from models r_{c_6} and r_{c_7} marginally underestimated BREBS-measured E_{Ta} by only 1%, performing better than the models r_{c_1}, r_{c_2}, r_{c_3}, r_{c_4}, and r_{c_5}, which overestimated BREBS-measured E_{Ta} by 17%, 18%, 16%, 16%, 16%, and 16%, respectively. The E_{Ta} predicted with r_c models r_{c_6} and r_{c_7} had a mean of 0.52 which was closely similar to the mean of measured E_{Ta} (0.53 mm h^{-1}). The means of E_{Ta} predicted with canopy resistance estimated from models r_{c_1}, r_{c_2}, r_{c_3}, r_{c_4}, and r_{c_5} were 0.61, 0.62, 0.61, 0.61, and 0.61 mm h^{-1}, respectively. The E_{Ta} predicted using r_{c_6} and r_{c_7} had a standard deviation of 0.24 mm h^{-1} which was less than the standard deviation of the other five models (0.27 mm h^{-1}).

[31] Unlike the results of r_c validation in 2006, the 2005 results clearly demonstrate that estimating E_{Ta} using r_c estimated from models r_{c_6} and r_{c_7} performed better than using the rest of the models. However, models r_{c_6} and r_{c_7} overestimated observed r_c (Figures 6f and 6g, respectively). Thus, one would have expected these models to estimate lower E_{Ta} as compared with the BREBS-measured E_{Ta}, but the E_{Ta} estimates of both models were within 1% of the BREBS E_{Ta}. This may be due to the combination of three reasons. First, it is likely that the PM model overestimated E_{Ta}, but since the r_{c_6} and r_{c_7} models were producing lower E_{Ta} due to overestimation of r_c, this offset the overestimation by the PM model as compared with the BREBS measurements. *Steduto et al.* [2003] and *Rana et al.* [1994] showed that the PM equation overestimates in cases with low ET values. *Perez et al.* [2006], *Zhang et al.* [2008], and *Irmak and Mutiibwa* [2009] showed that the PM equation can overestimate E_{Ta} during full canopy cover, especially during periods of high evaporative atmospheric demand. This is because during complete canopy cover and especially during periods with high evaporative atmospheric demand conditions when there is available soil water supply, the variable r_c approach in the PM model assigns a small resistance value which is assumed to be homogeneous for the whole canopy when in reality some leaves in the canopy are shaded and/or aged and may not contribute to the transpiration rate at the same level as the sunlit and young leaves [*Irmak and Mutiibwa*, 2009]. Younger and sunlit leaves would have lower r_c values than the older and shaded leaves, thus, transpiring at different levels and contributing differently to the total evaporative losses estimated by the PM model. It would be expected that the E_{Ta} rate estimated from the PM model to be less than those measured values. Thus, the E_{Ta} measured by the BREBS may better represent the total evaporative losses from the whole canopy accounting for E_{Ta} from various levels of shading and leaves with different ages.

[32] The second possible explanation is, especially in relation to the performance of the PM model in high atmospheric demand conditions, that the r_c may have been underestimated by models r_{c_6} and r_{c_7} in our case rather than the PM model itself overestimating during high evaporative demand conditions. The underestimation of r_c in our case might be due to not accounting for the VPD by *Irmak et al.*

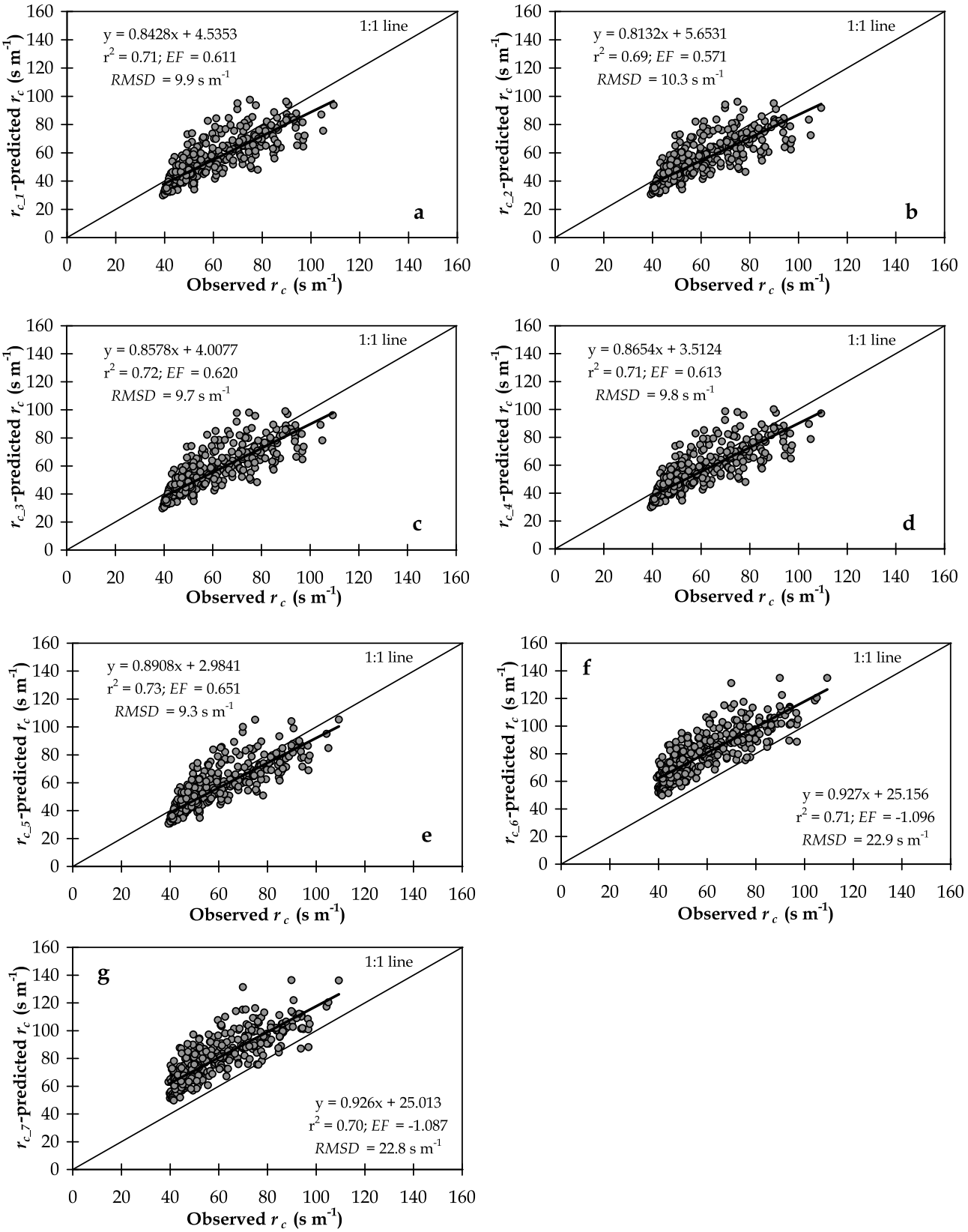

Figure 6. Validation (16 July to 31 August 2006) performance results for the seven canopy resistance (r_c) models (n = 405 for each case).

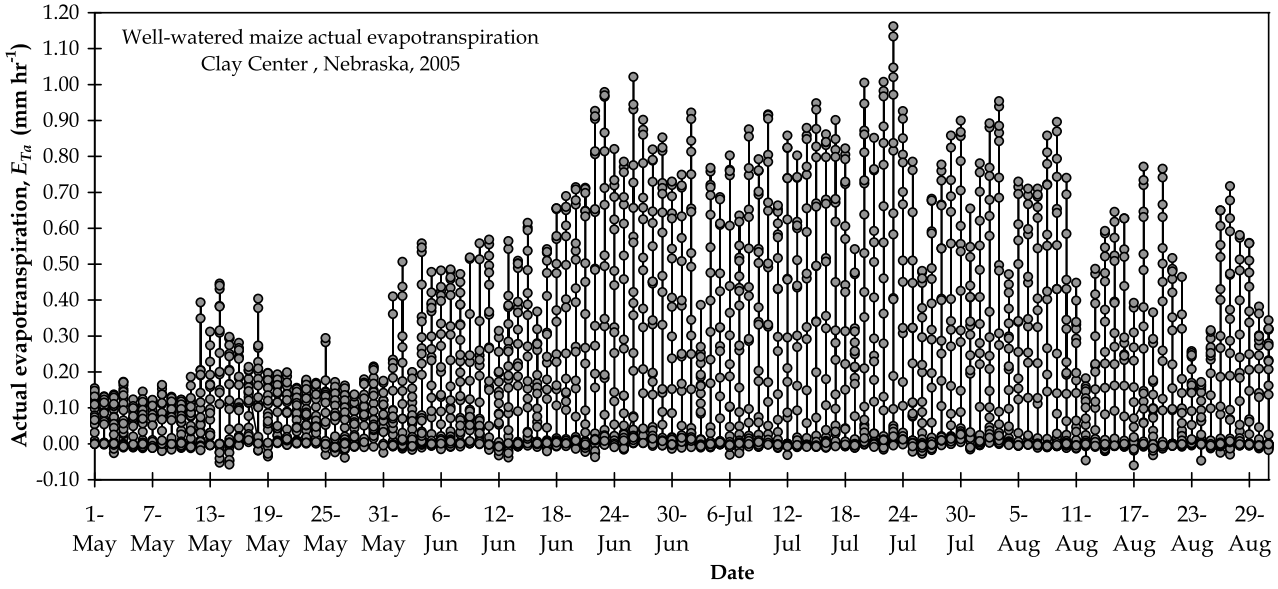

Figure 7. Seasonal (1 May to 31 August 2005) distribution of Bowen ratio energy balance system (BREBS)-measured hourly actual evapotranspiration (E_{Ta}) for well-watered maize canopy (n = 2952).

[2008] during the scaling-up r_s to r_c process, which is especially important during high evaporative demand settings. Furthermore, some variables may have been misestimated due to experimental and instrumental errors. Relative humidity, for example, is never perfectly estimated [*Ewers and Oren*, 2000] and the R_n measurements may not have been perfect. In addition, the BREBS-measured E_{Ta} contains some measurement error as well. The third possible explanation is the potential insensitivity of E_{Ta} to r_c. It has been suggested that E_{Ta} is estimated more accurately than estimated r_c because E_{Ta} depends only in part on r_c [*Stewart*, 1988; *Stewart and Gay*, 1989; *Gash et al.*, 1989]. The sensitivity analyses by *Finnigan and Raupach* [1987], *Stewart* [1988], and *Gash et al.* [1989] indicate that the E_{Ta} is fairly insensitive to r_c for agronomical plants. If the E_{Ta} is insensitive to r_c, then the better performance of models r_{c_6} and r_{c_7} in estimating E_{Ta} could be an artifact of a random performance based on the 2005 E_{Ta} and climate data set. We further tested this by evaluating the sensitivity of E_{Ta} to r_c for our data set in the next section.

3.7. Sensitivity of PM Model to r_c

[33] Figure 9 presents the change in E_{Ta} (mm h^{-1}) as estimated from the PM model per 10 s m^{-1} increase in observed r_c. The cumulative percent change in PM-estimated E_{Ta} versus changes in r_c for a morning and noon hour of the same day are also included in the same figure. While we kept all the variables constant during the analyses, we conducted the sensitivity analyses for a randomly selected day (19 June), and analyzed the sensitivity of E_{Ta} to r_c for a morning hour (09:00 am) and a noon hour (1:00 pm) for the same day to asses whether the E_{Ta} shows different response in two different microclimatic conditions for a canopy in the same environment. The observed r_c was increased from zero to 300 s m^{-1} with 10 s m^{-1} increments, and the E_{Ta} rate and the percent change in E_{Ta} from the PM model were calculated for both hours. The initial (base) E_{Ta} and r_c values along with the other microclimatic variables measured at 09:00 am and 1:00 pm are presented in Table 3. The response of E_{Ta} to changes in r_c was similar for morning and noon hours with decreasing trend in E_{Ta} as r_c increased. With the initial r_c (185 s m^{-1} for 09:00 am and 100 s m^{-1} for 1:00 PM) and other measured microclimatic variables, the PM-estimated E_{Ta} at 09:00 and 1:00 pm, respectively, were 0.09 mm h^{-1} and 0.46 mm h^{-1}. A unit (10 s m^{-1}) increase in r_c had slightly higher decrease in E_{Ta} for 1:00 pm, and the exponent of the E_{Ta} versus r_c lines for 1:00 pm was slightly higher (−0.0041) than the one for 09:00 am (−0.0043) (Figure 9). The *a* values in the exponential functions (equations are not shown on Figure 9) (0.738 and 0.2203) are analogous to an intercept because these are the values of the functions when $X = 0$ since exp(0) = 1. Since the exponents are similar, *a* value is more influential on the rate of change (the derivatives of the exponential functions) in E_{Ta}. The magnitude of the average rate of change in E_{Ta} at 1:00 pm was greater [−0.001744 mm h^{-1} decrease in E_{Ta} (negative sign indicates decrease) per 1 s m^{-1} increase in r_c] than for 09:00 am (−0.00053 mm h^{-1} decrease in E_{Ta} per 1 s m^{-1} increase in r_c). E_{Ta} did not respond to changes in r_c after about 210 s m^{-1} in the morning and after 270 s m^{-1} at 1:00 pm. Even though the rate of change was greater for the 1:00 pm curve, a unit increase in r_c had slightly higher percentage decrease in E_{Ta} in the morning. This is due to the solar radiation being significantly higher at noon than in the morning (888 versus 283 W m^{-2}). Since the solar radiation is the primary regulator of r_c, when there is sufficient light to keep stomata fully open, a unit increase in r_c would be expected to have lower impact on E_{Ta} under the same amount of radiation when the radiation is kept constant. This is because the role of other environmental variables in controlling stomata would be greater when there is no sufficient light in the morning.

[34] The cumulative percent change in E_{Ta}, reached −286% for morning and −262% at 1:00 pm (Figure 9) with

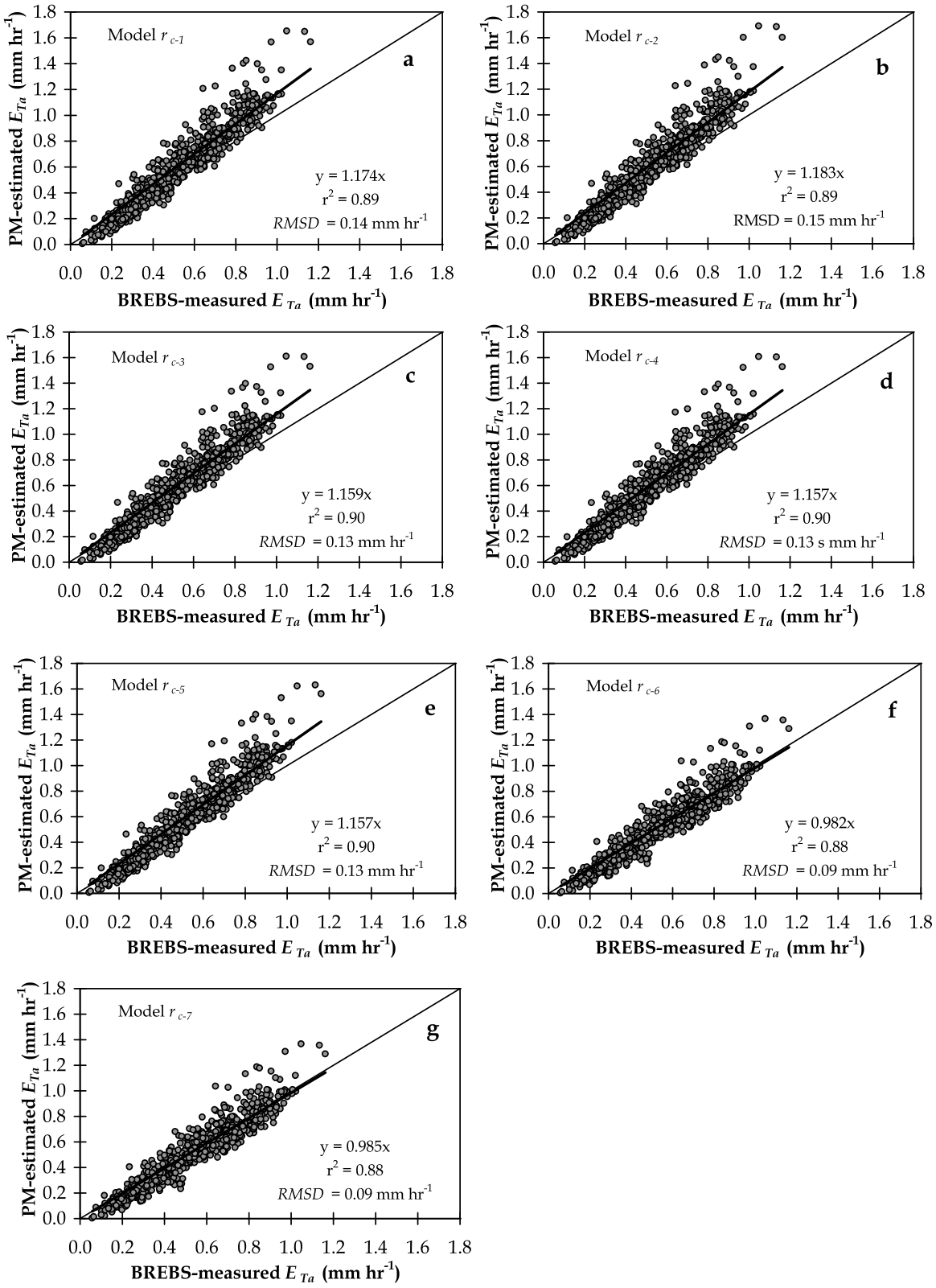

Figure 8. Comparison of Penman-Monteith (PM)-estimated hourly actual evapotranspiration (E_{Ta}), using estimated canopy resistance (r_c) from the seven models developed in this study, and the Bowen ratio energy balance system (BREBS)-measured hourly E_{Ta} for a well-watered maize canopy.

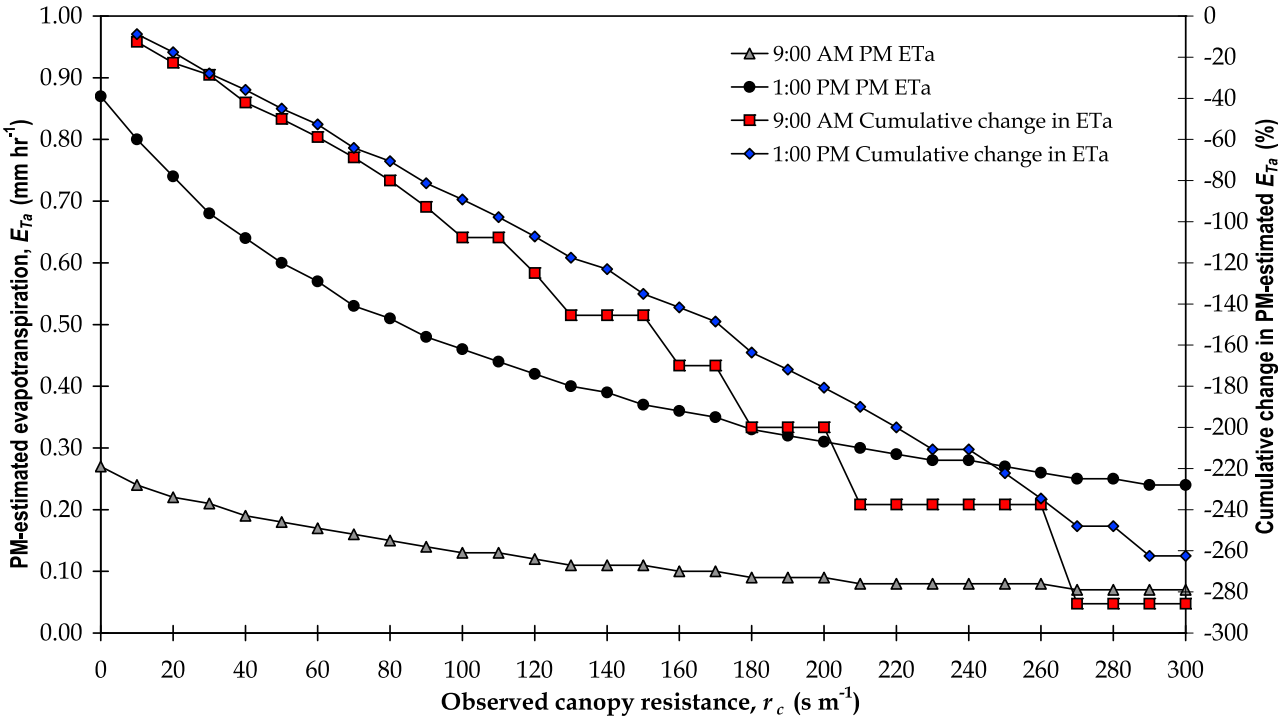

Figure 9. Response of Penman-Monteith (PM) model-estimated actual evapotranspiration (E_{Ta}) to changes in canopy resistance (r_c) for a morning and noon hour of the same day (19 June 2006) for a non-stressed maize canopy and cumulative percent change in Penman-Monteith (PM) model-estimated actual evapotranspiration (E_{Ta}) versus changes in canopy resistance (r_c) for a morning and noon hour of the same day (19 June 2006) for a nonstressed maize canopy.

the negative sign indicating decrease in E_{Ta}. In total, the E_{Ta} decreased from 0.27 to 0.07 mm at 09:00 am and from 0.87 to 0.24 mm h^{-1} at 1:00 pm when r_c increased from 0 to 300 s m^{-1}. Until 100 s m^{-1}, the response of E_{Ta} to change in r_c was never zero and was very similar for both the morning and noon hour (Figure 9). After 100 s m^{-1} for the morning and 200 s m^{-1} for the noon hour, the PM model sometimes showed no response (zero decrease in E_{Ta}) to increase in r_c every 10 or 20 s m^{-1}; thus, E_{Ta} response fluctuated in a wider range for the morning hour. Zero decrease in E_{Ta} was observed only three times for 1:00 pm at higher r_c values (240, 280, and 300 s m^{-1}). While we conducted the sensitivity analyses for only 1 day with morning and noon hours, the sensitivity of the PM E_{Ta} may show variation with time of the season due to changes in canopy and due to aerodynamic and energy terms of the model showing different sensitivities to dynamic micrometeorological conditions. However, while the magnitude of the sensitivity of the model may show variations, the trend and the relative sensitivity of the PM E_{Ta} to r_c should be similar throughout the season.

[35] To evaluate the relationship between observed r_c and E_{Ta} throughout the season in 2006, we graphed observed scaled-up hourly r_c values against BREBS-measured hourly E_{Ta} in Figure 10 and found a strong relationship between the two variables. The r_c and E_{Ta} data points in Figure 10 include those measured diurnally, usually from 09:00 am to 5:00 or 6:00 pm, from 19 June through 31 August 2006. The relationship was explained with an exponential decay function ($Y = ae^{-bx}$; $a = 2.414$ and $b = 0.0274$). On an hourly time step, r_c alone was able to explain 54% of the variability ($r^2 = 0.54$) in E_{Ta}, further indicating a strong dependence of E_{Ta} on r_c. The terms a and b had standard deviation of 0.1435 and 0.0011, respectively, with both terms being statistically significant ($P < 0.0001$). Figure 10 shows that most of the higher E_{Ta} rates were observed at the lower r_c range (40 to 100 s m^{-1}). The E_{Ta} rate decreased gradually as r_c increased. The highest BREBS-measured E_{Ta} rate (1.28 mm h^{-1}) occurred when observed r_c was 44.3 s m^{-1}. The higher r_c and lower E_{Ta} values in Figure 11 were observed in early morning hours and cloudy days with low solar radiation. These results and the sensitivity analy-

Table 3. Measured Environmental Variables at 09:00 am and 1:00 pm Where the Sensitivity of Penman-Monteith-Estimated Actual Evapotranspiration to Canopy Resistance was Determined[a]

Measured Variable	Unit	09:00 am	1:00 pm
T_a	°C	19.4	25.8
R_s	W m^{-2}	283.2	888.4
R_n	W m^{-2}	200.0	638.9
G	W m^{-2}	19.4	63.8
VPD	KPa	0.31	1.02
RH	%	85.7	68.4
r_a	s m^{-1}	29.8	27.3
u_3	m s^{-1}	2.5	4.1
u_3 direction	Degrees	East-southeast	East
Base r_c	s m^{-1}	185	100
Base E_{Ta}	mm h^{-1}	0.09	0.46

[a]The variables included air temperature (T_a), incoming shortwave radiation (R_s), net radiation (R_n), soil heat flux (G), vapor pressure deficit (VPD), relative humidity (RH), aerodynamic resistance (r_a, calculated from equation 1), wind speed at 3 m (u_3), wind direction, and base values for r_c and E_{Ta}.

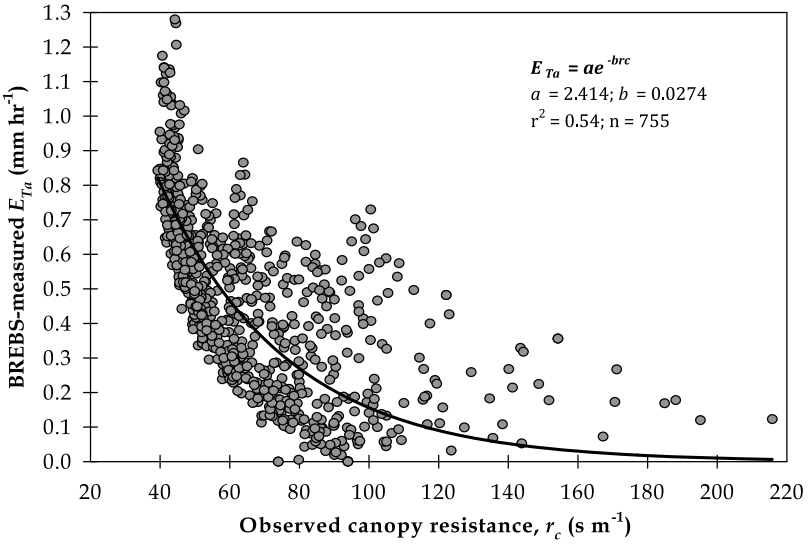

Figure 10. Relationship between observed scaled-up canopy resistance (r_c) and Bowen ratio energy balance system (BREBS)-measured actual evapotranspiration (E_{Ta}) for a nonstressed maize canopy. The r_c values were obtained from measured and scaled-up leaf stomatal resistance values as reported by *Irmak et al.* [2008] and *Irmak and Mutiibwa* [2009].

ses demonstrate that the PM-estimated E_{Ta} is very sensitive to changes in r_c, but this response is dynamic and is impacted by other factors, but more so by the amount of light (radiation). Thus, it appears that the good performance of model r_{c_6} and r_{c_7} in Figure 8 is most likely due to the overestimation of the PM model, likely due to underestimation of r_c by models r_{c_6} and r_{c_7}, as compared with the BREBS-measured E_{Ta} and not due to the insensitivity of the E_{Ta} to r_c.

[36] Figures 9 and 10 investigate the sensitivity of the PM E_{Ta} to r_c implicitly. To explicitly determine the sensitivity of the PM model-estimated E_{Ta} to r_c, we solved the following equation (all variables have been previously defined in equation 14):

$$\frac{\partial \lambda E_{Ta}}{\partial r_c} = \frac{\gamma\left(\Delta(R_n - G) + \rho c_p \frac{e_s - e_a}{r_a}\right)}{r_a\left(\Delta + \gamma\left(1 + \frac{r_c}{r_a}\right)\right)^2}. \qquad (16)$$

The ratio of $\partial \lambda E_{Ta}/\partial r_c$ essentially represents the sensitivity coefficients of the PM with respect to r_c. We plotted the hourly ratios (09:00 am to 6:00 pm) as a function of time in Figure 11. Daily average ratios also included in the figure. The hourly ratios ranged from near zero to 0.016 with a

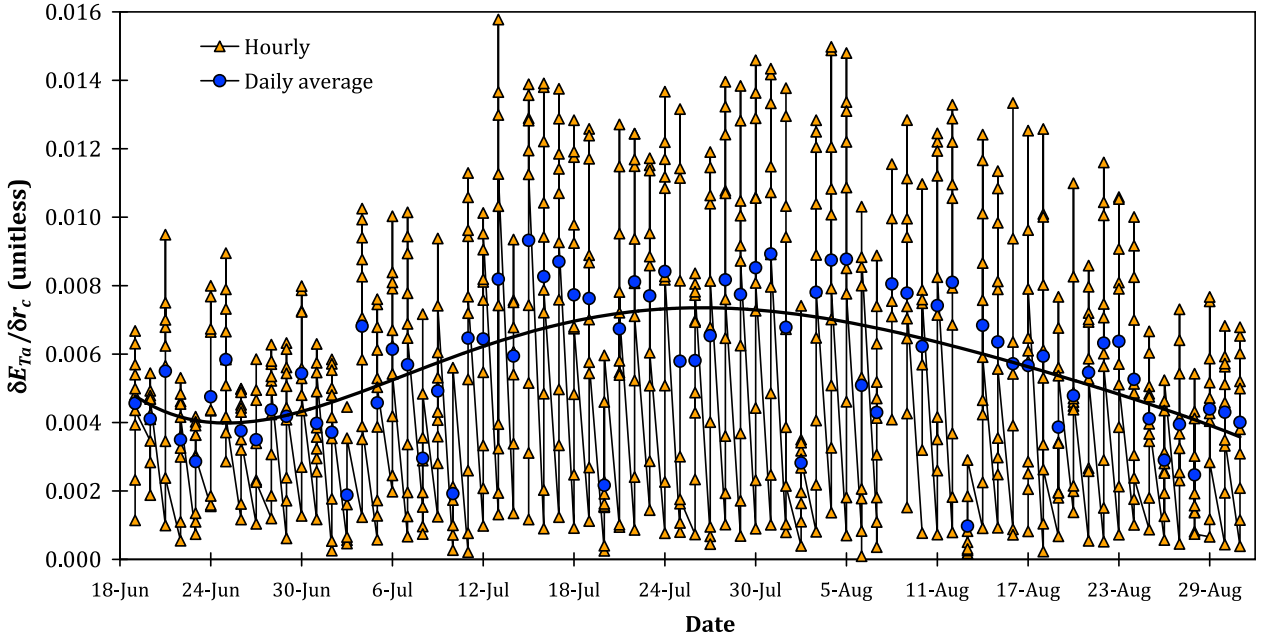

Figure 11. Sensitivity of the Penman-Monteith (PM) model to canopy resistance (r_c) ($\lambda E_{Ta}/r_c$, equation 16).

seasonal average of 0.006. The ratio was lowest early in the morning, was at maximum during midday, and started to decrease toward late afternoon. This diurnal trend is due to response of r_c to increase magnitude of the radiation, temperature, and other micrometeorological variables with time. The ratios were lower early in the season and largest in midseason during complete canopy cover and maximum LAI from mid-July to early August and decreased again toward the end of the season. The lower values in the late season is most likely due to insensitivity of the PM model to r_c as a result of physiological maturity and leaf senescence as the influence of the r_c on E_{Ta} is minimal in these conditions.

4. Conclusions

[37] We investigate the relationships between primary micrometeorological parameters and canopy resistance (r_c) and present seven models using a generalized-linear model approach to estimate r_c for a nonstressed maize canopy. The most complex r_c model uses net radiation (R_n), air temperature (T_a), vapor pressure deficit (VPD), relative humidity (RH), wind speed at 3 m (u_3), aerodynamic resistance (r_a), leaf area index (LAI), and solar zenith angle (Θ) as inputs. The simplest model requires R_n, T_a, and RH. The relationship between r_c versus u_3, wind direction, and Θ was weak. There was a strong relationship between r_c and T_a. Although there was a general trend of increasing r_c with increasing RH, this relationship was not strong. While the relationship between r_c and u_3 is not very clear, there was a tendency of increasing r_c with increasing u_3. The highest r_c values were obtained in the u_3 range of 2 to 4 m s^{-1}. The relationship between the r_c and LAI is inverse and is the strongest among all variables. Upon validation, the r_c model that used R_n, T_a, RH, u_3, and LAI had the best agreement with the observed r_c data. Exclusion of LAI resulted in reduced performance and exclusion of r_a and Θ from models did not impact the performance of the r_c models. The BREBS-measured and the PM-estimated E_{Ta}, using modeled r_c, were in close agreement. Given that most of the micrometeorological variables needed for the r_c models could be measured with a typical weather station, and the physiological variables, such as LAI, could be estimated with a reasonable accuracy, the performance obtained from all r_c models is an encouraging step toward empirical modeling of r_c for one-step application of the PM model for estimating E_{Ta} for nonstressed maize canopy. The purpose of the study was not to rank the models but rather to present empirical models predicting r_c with different numbers of environmental variables and evaluate their performances to better understand the impact of different environmental variables on r_c. Our findings could aid in the selection of a suitable model based on the availability and quality of the input data to predict r_c for one-step application of the PM model to estimate E_{Ta}.

References

Adams, R. S., T. A. Black, and R. L. Fleming (1991), Evapotranspiration and surface conductance in a high elevation, grass-covered forest clearcut, *Agric. For. Meteorol*, *56*, 173–193.

Alves, I., and L. S. Pereira (2000), Modeling surface resistance from climatic variables?, *Agric. Water Manage.*, *42*, 371–385.

Alves, I., A. Pereira, and L. S. Pereira (1998), Aerodynamic and surface resistance of complete cover crops: how good is the "big leaf"?, *Trans. ASAE*, *41*(2), 345–351.

Aphalo, P. J., and P. G. Jarvis (1991), Do stomata respond to relative humidity?, *Plant Cell Environ.*, *14*, 127–132.

Bailey, W. G., and J. A. Davies (1981), Bulk stomatal resistance control on evaporation, *Boundary Layer Meteorol.*, *20*, 401–415.

Baldocchi, D. D., R. J. Luxmoore, and J. L. Hatfield (1991), Discerning the forest from the trees: An essay on scaling canopy stomatal conductance, *Agric. For. Meteorol.*, *54*, 197–226.

Ball, J. T., I. E. Woodrow, and I. A. Berry (1987), A model predicting stomatal conductance and its contribution to the control of photosynthesis under different environmental conditions, in *Progress in Photosynthesis Research*, edited by J. Biggins, vol. IV, pp. 221–224, Martinus Nijhoff, Amsterdam, Netherlands.

Beadle, C. L., H. Talbot, R. E. Neilson, and P. G. Jarvis (1985), Stomatal conductance and Photosynthesis in a mature scots pine forest. III. Variation in canopy conductance and canopy photosynthesis, *J. Appl. Ecol.*, *22*, 587–595.

Brutsaert, W., and H. Stricker (1979), An advective-aridity approach to estimate actual regional evapotranspiration, *Water Resour. Res.*, *15*(2), 443–450.

Brutsaert, W. H. (1982), *Evaporation Into Atmosphere*, D. Reidel, Dordrecht, Holland.

Campbell, G. S. (1982), Fundamentals of radiation and temperature relations, in *Physiological Plant Ecology, I: Responses to the Physical Environment*, edited by O. L. Lange, *Encyclopedia of Plant Physiology*, vol. 12a, pp. 11–40, Springer, New York.

Collatz, G. J., J. T. Ball, C. Grivet, and J. A. Berry (1991), Physiological and environmental regulation of stomatal conductance, photosynthesis and transpiration: A model that includes a laminar boundary layer, *Agric. For. Meteorol.*, *54*, 107–136.

Ehleringer, J. R., and C. B. Field (Eds.) (1993), *Scaling Physiological Processes: Leaf to Globe*, Academic, New York.

Ewers, B. E., and R. Oren (2000), Analysis of assumptions and errors in the calculation of stomatal conductance from sap flux measurements, *Tree Physiol.*, *20*, 579–590.

Ewers, B. E., S. T. Gower, B. Bond-Lamberty, and C. K. Wang (2005), Effects of stand age and tree species on canopy transpiration and average stomatal conductance of boreal forests, *Plant Cell Environ.*, *28*(5), 660–678.

Ewers, B. E., R. Oren, H. S. Kim, G. Bohrer, and C. T. Lai (2007), Effects of hydraulic architecture and spatial variation in light on mean stomatal conductance of tree branches and crowns, *Plant Cell Environ.*, *30*(4), 483–496.

Ewers, B. E., D. S. Mackay, J. Tang, P. V. Bolstad, and S. Samanta (2008), Intercomparison of sugar maple (*Acer saccharum* Marsh.) stand transpiration responses to environmental conditions from the Western Great Lakes Region of the United States, *Agric. For. Meteorol.*, *148*(2), 231–246.

Finnigan, J. J., and M. R. Raupach (1987), Modern theory of transfer in plant canopies in relation to stomatal characteristics, in *Stomatal Physiology*, edited by E. Zeiger, G. D. Farquhar, and I. R. Cowan, pp. 385–429, Stanford Univ. Press, Calif.

Franks, P. J. (2004), Stomatal control and hydraulic conductance, with special reference to tall trees, *Tree Physiol.*, *24*, 865–878.

Gash, J. H. C., W. J. Shuttleworth, C. R. Lloyd, J. C. Andre, J. P. Goutorbe, and J. Gelpe (1989), Micrometeorological measurements in Les Landes forest during HAPEX-MOBILHY, *Agric. For. Meteorol.*, *73*, 131–147.

Ham, J. M., and J. L. Heilman (1991), Aerodynamic and surface resistances affecting energy transport in a sparse crop, *Agric. For. Meteorol.*, *53*, 267–284.

Irmak, A., and S. Irmak (2008), Reference and crop evapotranspiration in south central Nebraska: II. Measurement and estimation of actual evapotranspiration, *J. Irrig. Drain. Eng.*, *134*(6), 700–715.

Irmak, S., and D. Mutiibwa (2008), Dynamics of photosynthetic photon flux density and light extinction coefficient for assessing radiant energy interactions for maize canopy, *Trans. ASABE*, *51*(5), 1663–1673.

Irmak, S., and D. Mutiibwa (2009), On the dynamics of stomatal resistance: Relationships between stomatal behavior and micrometeorological variables and performance of Jarvis-type parameterization, *Trans. ASABE*, *52*(6), 1923–1939.

Irmak, S., D. Mutiibwa, A. Irmak, T. J. Arkebauer, A. Weiss, D. L. Martin, and D. E. Eisenhauer (2008), On the scaling up leaf stomatal resistance to canopy resistance using photosynthetic photon flux density, *Agric. For. Meteorol.*, *148*, 1034–1044.

Jarvis, P. G. (1976), The interpretation of the variations in leaf water potential and stomatal conductance found in canopies in the field, *Phil. Trans. R. Soc. London, Ser. B.*, *273*, 593–610.

Jarvis, P. G. (1981), Stomatal conductance, gaseous exchange and transpiration, in *Plants and Their Atmospheric Environment*, edited by J. Grace, E. D. Ford, and P. G. Jarvis, pp. 175–204, Blackwell Sci., Oxford, U. K.

Jarvis, P. G., and K. G. McNaughton (1986), Stomatal control of transpiration: Scaling up from leaf to region, *Adv. Ecol. Res.*, *15*, 1–49.

Juang, J.-Y., G. G. Katul, M. B. Siqueira, P. C. Stoy, and H. R. McCarthy (2008), Investigating a hierarchy of Eulerian closure models for scalar transfer inside forested canopies, *Boundary Layer Meteorol.*, *128*, 1–32, doi:10.1007/s10546-008-9273-2.

Katul, G. G., Leuning, and R. Oren (2003), Relationship between plant hydraulic and biochemical properties derived from a steady-state coupled water and carbon transport model, *Plant Cell Environ.*, *26*, 339–350.

Katul, G. G., S. Manzoni, S. Palmroth, and R. Oren (2009a), A stomatal optimization theory to describe the effects of atmospheric CO_2 on leaf photosynthesis and transpiration, *Ann. Bot.*, *1–12*, doi:10.1093/aob/mcp292.

Katul, G. G., S. Palmroth, and R. Oren (2009b), Leaf stomatal responses to vapour pressure deficit under current and CO_2-enriched atmosphere explained by the economics of gas exchange, *Plant Cell Environ.*, *32*, 968–979, doi: 10.1111/j.1365-3040.2009.01977.x.

Kramer, P. J. (1983), *Water Relations of Plants*, pp. 489, Academic, New York.

Leuning, R., F. M. Kelliher, D. G. G. De Purry, and E. D. Schulze (1995), Leaf nitrogen, photosynthesis, conductance and transpiration: scaling from leaves to canopies., *Plant Cell Environ.*, *18*, 1183–1200.

Leverenz, J., J. D. Deans, E. D. Ford, P. G. Jarvis, R. Milne, and D. Whitehead (1982), Systematic spatial variation of stomatal conductance in a Sitka spruce plantations, *J. Appl. Ecol.*, *19*, 835–851

Lhomme, J. P. (1991), The concept of canopy resistance: Historical survey and comparison of different approaches, *Agric. For. Meteorol.*, *54*, 227–240.

Mackay, D. S., D. E. Ahl, B. E. Ewers, S. Samanta, S. T. Gower, and S. N. Burrows (2003), Physiological tradeoffs in the parameterization of a model of canopy transpiration, *Adv. Water Res.*, *26*(2), 179–194.

Massman, W. J., and M. R. Kaufmann (1991), Stomatal response to certain environmental factors: a comparison of models for subalpine trees in the Rocky Mountains, *Agric. For. Meteorol.*, *54*, 155–167.

McCullagh, P., and J. A. Nelder (1989), *Generalized Linear Models*, 2nd ed., Chapman and Hall, London.

McNaughton, K. G., and P. G. Jarvis (1983), Predicting effects of vegetation changes on transpiration and evaporation, in *Water Deficits and Plant Growth*, edited by T. T. Kozlowski, vol. VII, pp. 1–47, Academic.

Meinzer, F. C., and D. A. Grantz (1990), Stomatal and hydraulic conductance in growing suga r_c ane-stomatal adjustment to water transport capacity, *Plant Cell Environ.*, *13*, 383–388.

Meinzer, F. C., G. Goldstein, P. Jackson, N. M. Holbrook, M. V. Gutierrez, and J. Cavlier (1995), Environmental and physiological regulation of transpiration in tropical forest gap species: the influence of boundary layer and hydraulic conductance properties, *Oceologia*, *101*, 514–522.

Monteith, J. L. (1965), Evaporation and the environment, in *The State and Movement of Water in Living Organisms, XIXth Symposium*, pp. 205–234, Cambridge Univ. Press, Cambridge, U.K.

Monteith, J. L. (1995), Accommodation between transpiring vegetation and the convective boundary layer, *J. Hydrol.*, *166*, 251–263.

Monteith, J. L., and M. Unsworth (1990), *Principles of environmental physics*, 2nd ed., Edward Arnold, London, England.

Monteith, J. L., G. Szeicz, and P. E. Waggoner (1965), The measurement and control of stomatal resistance in the field, *J. Appl. Ecol.*, *2*, 345–355.

Mott, K. A., and D. F. Parkhurst (1991), Stomatal response to humidity in air and helox, *Plant Cell Environ.*, *14*, 509–515.

Norman, J. M. (1979), Modeling the complete crop canopy. Modification of the Aerial Environment of Plants (B. J. Barfield and J. F. Gerber, eds.), *Am. Soc. Agric. Eng. Monogr.*, *2*, 249–277.

Oren, R., J. S. Sperry, G. G. Katul, D. E. Pataki, B. E. Ewers, N. Phillips, and K. V. R. Schafer (1999), Survey and synthesis of intra- and interspecific variation in stomatal sensitivity to vapour pressure deficit, *Plant Cell Environ.*, *22*, 1515–1526.

Pataki, D. E., and R. Oren (2003), Species differences in stomatal control of water loss at the canopy scale in a mature bottomland deciduous forest, *Adv. Water Res.*, *26*(12), 1267–1278.

Penman, H. L. (1948),Natural evaporation from open water, bare soil, and grass, *Proc. R. Soc. London, Ser. A*, *193*, 120–145.

Perez, P. J., S. Lecina, F. Castellvi, A. Martinez-Cob, and F. J. Villalobos (2006), A simple parameterization of bulk canopy resistance from climatic variables for estimating hourly evapotranspiration, *Hydrol. Processes*, *20*, 515–532.

Philip, J. R. (1966), Plant-water relations: some physical aspects, *Ann. Rev. Plant Physiol.*, *17*, 245–268.

Plate, E. J. (1971), Aerodynamic characteristics of atmospheric boundary layers, AEC Critical Review Series, U.S. Atomic Energy Commission, Div. Tech. Info. U.S. Gov. Print. Office, Washington, D. C.

Rana, G., N. Katerji, M. Mastrorilli, and ElM. Moujabber (1994), Evapotranspiration and canopy resistance of grass in a Mediterranean region, *Theor. Appl. Climatol.*, *50*, 61–71.

Rochette, P., R. L. Desjardins, L. M. Dwyer, D. W. Stewart, and P. A. Dube (1991), Estimation of maize (*Zea mays L.*) canopy conductance by scaling up leaf stomatal conductance, *Agric. For. Meteorol.*, *54*, 241–261.

Saliendra, N. Z., J. S. Sperry, and J. P. Comstock (1995), Influence of leaf water status on stomatal response humidity, hydraulic conductance, and soil drought in *Betula occidentalis*, *Planta*, *196*, 357–366.

Salisbury, F. B., and C. W. Ross (1992), *Plant Physiology*, 4th ed., Wadsworth, Belmont, Calif.

Seller, P. J., Y. Mintz, Y. C. Sud, and A. Dalcher (1986), A simple biosphere model (SiB) for use within general circulation models, *J. Atmos. Sci.*, *43*, 505–531.

Shuttleworth, W. J. (2006), Towards one-step estimation of crop water requirements, *Trans. ASABE*, *49*(4), 925–935.

Sinclair, T. R., C. E. Murphey, and K. R. Knoerr (1976), Development and evaluation of simplified models simulating canopy photosynthesis and transpiration, *J. Appl. Ecol.*, *13*, 813–829.

Sperry, J. S. (2000), Hydraulic constrains on plant gas exchange, *Agric. For. Meteorol.*, *104*, 13–23.

Sperry, J. S., and W. T. Pockman (1993), Limitation of transpiration by hydraulic conductance and xylem cavitation in Betula occidentalis, *Plant Cell Environ.*, *16*, 279–288.

Sperry, J. S., N. N. Alder, and S. E. Eastlack (1993), The effect of reduced hydraulic conductance on stomatal conductance and xylem cavittaion, *J. Exp. Bot.*, *44*, 1075–1082.

Sperry, J. S., F. R. Adler, G. S. Campbell, and J. P. Comstock (1998), Limitation of plant water use by rhizosphere and xylem conductance: results from model, *Plant Cell Environ.*, *21*, 347–359.

Steduto, P., M. Todorovic, A. Calandro, and P. Rubino (2003), Daily ETo estimates by the Penman-Monteith equation in Southern Italy: Constant versus variable canopy resistance, *Theor. Appl. Climatol.*, *74*, 217–225.

Stewart, J. B. (1988), Modeling surface conductance of pine forest, *Agric. For. Meteorol.*, *43*, 19–35.

Stewart, J. B., and L. W. Gay (1989), Preliminary modeling of transpiration from the FIFE site in Kansas, *Agric. For. Meteorol.*, *48*, 305–315.

Szeicz, G., and I. F. Long (1969), Surface resistance of crop canopies, *Water Resour. Res.*, *5*(3), 622–633.

Tanner, C. B. (1963), Basic instrumentation and measurements for plant environment and micrometeorology, *Soils Bull.*, *6*, Dep. of Soil Sci., Univ. of Wisconsin, Madison.

Thom, A. S. (1975), Momentum, Mass and heat exchange of plant communities, in *Vegetation and the atmosphere*, edited by J. L. Monteith, vol. 1, pp. 57–109, Academic Press, London.

Webb, E. K. (1984), Evaluation of evapotranspiration and canopy resistance: An alternative combination approach, *Agric. Water Manage.*, *8*, 151–166.

Whitehead, D. (1998), Regulation of stomatal conductance and transpiration in forest canopies, *Tree Physiol. 18*, 633–644.

Whitehead, D., and P. G. Jarvis (1981), Coniferous forests and plantations, in *Water deficits and Plant growth*, edited by T. T. Kozlowski, pp. 49–152, Academic, New York.

Whitehead, D., P. G. Jarvis, and R. H. Waring (1984), Stomatal conductance, transpiration and resistance to uptake in a *Pinus sylvestris* spacing experiment, *Can. J. For. Res.*, *14*, 692–700.

Zhang, B., S. Kang, F. Li, and L. Zhang (2008), Comparison of three evapotranspiration models to Bowen ratio-energy balance method over a vineyard in an arid desert region of northwest China, *Agric. For. Meteorol.*, *148*, 1629–1640.

S. Irmak and D. Mutiibwa, Department of Biological Systems Engineering, University of Nebraska-Lincoln, 241 L.W. Chase Hall, Lincoln, NE 68583, USA. (sirmak2@unl.edu)